

# European Facility for Antiproton and Ion Research (FAIR): the new international center for fundamental physics and its research program

V E Fortov, B Yu Sharkov, H Stöcker

DOI: 10.3367/UFNe.0182.201206c.0621

## Contents

<b>1. Introduction</b>	<b>582</b>
<b>2. Accelerator complex</b>	<b>583</b>
2.1 Accelerator concept and arrangement of the main systems; 2.2 Collector, storage, and cooling rings. Preparation of beams	
<b>3. Structure of atomic nucleus, astrophysics, and nuclear reactions with rare-isotope beams: NuSTAR experiment</b>	<b>586</b>
<b>4. Dense baryon matter: the CBM experiment</b>	<b>588</b>
4.1 CBM scientific program; 4.2 CBM detector	
<b>5. Antiproton annihilation: the PANDA experiment</b>	<b>589</b>
5.1 Physics program with antiproton beams; 5.2 PANDA detector	
<b>6. Physics of high energy density in matter: plasma physics</b>	<b>593</b>
6.1 HIHEX experiment; 6.2 LAPLAS experiment; 6.3 WDM experiment	
<b>7. Atomic physics with relativistic beams of highly charged ions and antiprotons</b>	<b>598</b>
<b>8. Atomic physics at a facility for low-energy antiproton and ion research (FLAIR)</b>	<b>599</b>
<b>9. Radiative study of materials and biophysics (BIOMAT)</b>	<b>599</b>
9.1 Biophysical experiments; 9.2 Experiments in material science; 9.3 Experiments on the modification of materials by relativistic heavy ion beams	
<b>10. Conclusions</b>	<b>601</b>
<b>References</b>	<b>601</b>

**Abstract.** The Facility for Antiproton and Ion Research (FAIR) accelerator center at Darmstadt, Germany, will provide the international scientific community with unique experimental opportunities of a scope and scale out of reach for any other large-scale facility in the world. With its staff of over 2500, it is expected to fundamentally expand our knowledge of hadron, nuclear, and atomic physics and their application to cosmology, astrophysics, and technology. In this review, the design details of the accelerator complex are discussed and the experimental

research program for FAIR is presented. Particular attention is paid to experiments on the extreme state of matter arising from the isochoric heating of a material by heavy-ion beams. One of the largest facilities of its kind in Europe, FAIR is a part of the strategic development roadmap for the European Strategic Forum on Research Infrastructures (ESFRI).

## 1. Introduction

Exploration of the basic properties and the structure of matter as well as of the evolution of the Universe since its inception has always been one of the central problems of contemporary physics. Fundamentally new experimental data concerning the ambient matter, which form our outlook of the world, have always been and still are provided by the production of extreme states of matter in laboratory conditions along with observations of astrophysical objects. A special place among research facilities belongs to relativistic accelerators like the Large Hadron Collider (LHC) at CERN, the Relativistic Heavy Ion Collider (RHIC) at the Brookhaven National Laboratory, USA, and the cyclotron complex of the RIKEN Science Center, Japan, as well as the domestic accelerators TWAC-ITEP at the Alikhanov Institute for Theoretical and Experimental Physics (ITEP) and the Nuclotron at the Joint Institute for Nuclear Research (JINR) [1, 2].

**V E Fortov** Joint Institute for High Temperatures,  
Russian Academy of Sciences,  
ul. Izhorskaya 13, 125412 Moscow, Russian Federation  
E-mail: fortov@ras.ru

**B Yu Sharkov** Russian Federation State Scientific Center  
'Alikhanov Institute for Theoretical and Experimental Physics',  
ul. Bol'shaya Chermushkinskaya 25, 117218 Moscow,  
Russian Federation  
E-mail: boris.sharkov@itep.ru

**H Stöcker** GSI Helmholtzzentrum für Schwerionenforschung GmbH,  
Planckstr 1, 64291 Darmstadt, Germany

Received 11 May 2011, revised 20 December 2011

*Uspekhi Fizicheskikh Nauk* **182** (6) 621 – 644 (2012)

DOI: 10.3367/UFNe.0182.201206c.0621

Translated by E N Ragozin; edited by A M Semikhatov

The European Facility for Antiproton and Ion Research (FAIR) is the project of a new research complex around a multi-purpose accelerator with unrivaled antiproton and radioactive nuclei beam parameters, which open unique possibilities for the pursuance of research along topical lines of modern science.

The ultra-modern FAIR accelerator complex under construction in Darmstadt will provide high-energy, precisely aligned beams of antiprotons and different ions possessing a uniquely high quality (in brightness and phase density) and tremendous intensity. A distinctive feature of the complex under development is the capability of generating high-intensity primary and secondary beams of stable and radioactive nuclei, as well as of antiproton beams exceeding the presently available beams by a factor of 100–10000 in intensity.

Furthermore, experiments on FAIR will enable a substantial advancement in the investigation of unknown domains of the phase diagram of nuclear matter, which are unattainable in experiments on the RHIC and LHC being put into service [1], where primary emphasis is placed on investigations into the properties of nuclear matter at extremely high temperatures and low baryon densities. By contrast, the FAIR experiments are targeted at a detailed study of the properties of matter at the highest baryon densities attainable under terrestrial conditions.

The scientific program at the FAIR accelerator complex embraces the following lines of research.

- Study of nuclear structure and investigations in the area of nuclear astrophysics using the beams of stable ions and of short-lived (radioactive) nuclei away from the stability limit.
- Study of hadron structure, investigations aimed at elaboration and verification of the theory of strong interactions — quantum chromodynamics (QCD) — with the use of primarily antiproton beams.
- Construction of the phase diagram of nuclear matter, study of quark deconfinement and the quark–gluon plasma.
- Investigations into the physics of superdense electromagnetic plasma employing high-intensity pulsed heavy-ion beams in unique combination with petawatt laser radiation.
- Investigations in the area of atomic physics, quantum electrodynamics (QED) in ultrahigh electromagnetic fields with the use of antiproton and high-charge heavy-ion beams.
- Applied research involving ion beams for the radiative study of materials, medicine, and biology.

Realizing the necessary experimental conditions called for a quest for original engineering and technological solutions. The FAIR will use:

- new superconducting magnet designs for obtaining particle beams of highest possible intensity;
- original techniques for the precision control of the beam energy and geometry;
- large-scale detectors capable of tracing the trajectories and determining the parameters of the multitude of particles produced in experiments.

Huge data streams arriving from detectors call for new hardware and software solutions (like GRID technologies) for data processing, access, and storage.

The international FAIR project is among the base projects of the European Strategy Forum on Research Infrastructures (ESFRI) [3]. Fifteen countries are participating in the FAIR project: Austria, Great Britain, Germany, India, Spain, Italy, China, Poland, Russia, Romania, Slovakia, Slovenia, Finland, France, and Sweden, which intend to make contributions to the project in the form of

delivery of high-technology equipment and components of experimental facilities, as well as in the form of cash payments.

The total project cost, including construction, maintenance, and operating costs for the period up to 2025, amounts to about 3 billion euros. The cost of the startup phase of the accelerator center and its base research facilities exceeds 1.3 billion euros.

The FAIR facility construction period is determined to last eight years, with the completion of construction projected for 2018. However, the commencement of research on several subsystems of the accelerator complex is planned for 2017.

About 3000 researchers from all over the world are preparing for experiments at the FAIR accelerator complex, whose common objective is the study of the basic properties and structure of matter and the evolution of the Universe since its beginning. Presently, 14 big international collaborations have been set up, which are grouped into four topical lines of research:

- Nuclear STructure and AstRophysics (NuSTAR);
- Compressed Baryonic Matter (CBM);
- antiProton ANihilation in DArmstadt (PANDA);
- superdense plasma physics, atomic physics, as well as applied research in material science and biology — Atomic, Plasma Physics, and Applications (APPA).

We discuss each of the areas in greater detail in what follows.

## 2. Accelerator complex

The heavy-ion accelerator complex [4] operating in Gesellschaft für Schwerionenforschung, GSI, in Darmstadt is one of the most successfully operating facilities with a multidimensional program of international experiments. However, in 2002, a start was made on the conceptual development of a new-generation multi-purpose facility with new requirements for the quality and intensity of ion and antiproton beams intended for the pursuance of experimental investigations under previously unattainable conditions. In 2006, an international scientific community—2500 scientists and engineers from 44 countries—composed a FAIR baseline technical report detailing the engineering diagram and the components of the requisite accelerator system and the proposed types of experiments. The main special feature of FAIR is a complicated and economically sound arrangement of several accelerator systems, which is aimed at the production of particle beams with an unprecedentedly wide range of parameters. The most important virtue of the accelerator complex is that it will allow the simultaneous, parallel execution of up to five research programs. By and large, the complex will be operating for different experiments as if it were intended for each of them separately.

The main parameters of the FAIR accelerator complex and its general view are presented in Table 1 and Fig. 1. The existing UNiversal Linear ACcelerator (UNILAC) and the SIS-18 synchrotron (a heavy-ion synchrotron with a magnetic rigidity of 18 T m) will serve as injectors for the FAIR accelerator complex.

### 2.1 Accelerator concept and arrangement of the main systems

The FAIR complex consists of carefully designed, interconnected systems for the acceleration and storage of high-

**Table 1.** Main parameters of synchrotrons and storage rings.

Ring	Ring perimeter, m	Magnetic rigidity, T m	Beam energy
SIS-100 synchrotron	1084	100	2.7 GeV/nucleon, $^{238}\text{U}^{28+}$ 27 GeV, protons
SIS-300 synchrotron	1084	300	34 GeV/nucleon, $^{238}\text{U}^{92+}$
Collector Ring (CR)	211	13	0.74 GeV/nucleon, $^{238}\text{U}^{92+}$ 3 GeV, antiprotons
Recirculation Experimental Storage Ring (RESR)	245	13	0.74 GeV/nucleon, $^{238}\text{U}^{92+}$ 3 GeV, antiprotons
New Experimental Storage Ring (NESR)	222	13	0.74 GeV/nucleon, $^{238}\text{U}^{92+}$ 3 GeV, antiprotons
High Energy Storage Ring (HESR)	574	50	14 GeV, antiprotons

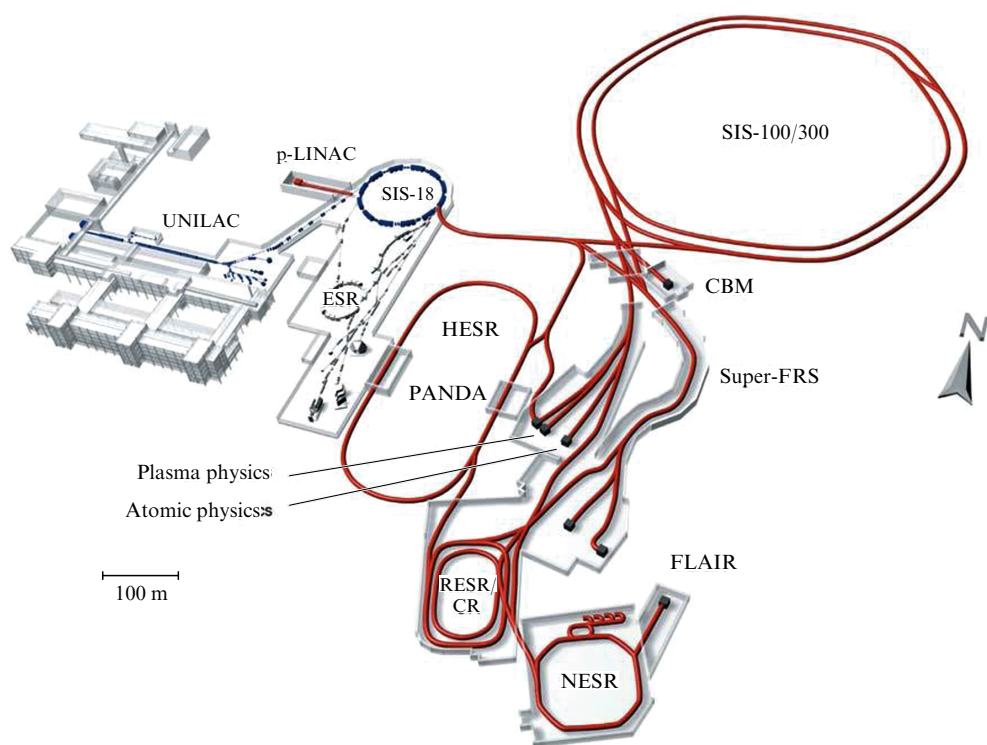


**Figure 1.** Schematic view of the FAIR accelerator complex. UNILAC, SIS-18, ESR (Experimental Storage Ring) are the presently existing facilities, FLAIR is the Facility of Low-Energy Antiproton and Heavy Ion Research, p-LINAC is the linear proton accelerator. For the interpretation of the remaining abbreviations and comments, see Table 1 and the text.

quality particle beams, as well as for the production of secondary particles by bombarding targets with primary beams. High-energy proton and ion beams will be used for producing secondary antiproton beams and stable and unstable (radioactive) nuclei. The secondary beams may either be used directly or be guided to a complex system of storage rings, where they will be formed into beams with the parameters required for experiments.

The basis for FAIR is made up of two accelerator synchrotron rings with perimeters of about 1100 m (SIS-100 and SIS-300) and respective magnetic rigidities of 100 and 300 T m located one above the other in an underground tunnel. These synchrotron rings are intended for the acceleration of different ions, from hydrogen ions (protons) to uranium ions. The presently operating UNILAC and SIS-18

accelerators will preliminarily accelerate ions prior to their injection into the new SIS-100 ring, intended for the generation of high-intensity pulsed ion beams for the purpose of their subsequent conversion to secondary beams of the nuclei of rare elements and for the proton-to-antiproton beam conversion. The synchrotron ring will consist of superconducting magnetic elements affording magnetic fields up to 4 T at a frequency of 1 Hz (ramp rate of  $4\text{ T s}^{-1}$ ). The rated intensity for  $\text{U}^{28+}$  uranium ions is equal to  $5 \times 10^{11}$  ions per pulse for a 1 GeV/nucleon energy and for protons, to  $4 \times 10^{13}$  protons per pulse for an energy of 29 GeV. A new linear proton accelerator designed for an energy of 70 MeV will be constructed for the injection of high-intensity proton beams.

Both ion and proton beams will undergo compression in pulse duration for the generation, storage, and subsequent

cooling of exotic nuclei and antiprotons with the respective pulse durations 60 and 25 ns. Short, high-intensity, heavy-ion bunches are also required in plasma physics experiments.

Also possible is a continuous beam mode with the average intensity of  $\approx 3 \times 10^{11}$  ions in 1 s and an energy of 1 GeV/nucleon with beam ejection either immediately from the SIS-100 ring or on beam transfer to the SIS-300 ring and the subsequent slow extraction from the latter.

Accelerated uranium nuclei will be injected into the SIS-300 ring constructed on the basis of superconducting fast-cycling magnetic elements, providing the field up to 6 T with the ramp rate  $1 \text{ T s}^{-1}$ . The maximum ion energy will amount to 45 GeV/nucleon for  $\text{Ne}^{10+}$  and to 34 GeV/nucleon for fully ionized  $\text{U}^{92+}$ . The beams will be slowly extracted with an intensity up to  $\sim 10^{10}$  particles per second with an extraction period of 10–100 ns for heavy nuclei collision experiments with the generation of superdense nuclear matter.

## 2.2 Collector, storage, and cooling rings.

### Preparation of beams

Transport lines connect the SIS-100 and SIS-300 accelerators to a complex system of subsequent rings. The bunches introduced into these rings are stored, ‘cooled’, and prepared for specific experiments. FAIR will operate in a multifunctional mode, permitting the simultaneous execution of up to five research programs with five different particle beams. This will be provided via coordinated beam control in both synchrotrons and adjacent storage and accelerator rings. Therefore, in each of the experiments, it will be possible to simultaneously use beams with the highest possible intensity.

Carrying out precision physical experiments requires that the secondary beams have specific energies and that all beam particles move in the same direction with the same velocity (minimal longitudinal phase volume). This is accomplished using different methods of beam cooling.

FAIR will employ two kinds of cooling:

— electron cooling (see, e.g., Ref. [4]), whereby ions are decelerated to a common velocity in the periodic interaction with a parallel beam of electrons that have a strictly defined velocity;

— stochastic cooling, whereby the so-called pickup electrodes determine the geometrical position of the bunch circulating in the ring for generating the requisite field amplitude of correction deflection kickers — pulsed devices for the fast control of bunches located at the diametrically opposite sections of the storage ring [5, 6].

The beams are cooled and prepared for experiments in the four subsequent rings.

- Collector Ring (CR), in which secondary ion and antiproton beams are subjected to stochastic cooling. This ring provides a lowering of the total phase volume by a factor of  $1.6 \times 10^4$  for an antiproton beam (the cooling period is equal to 10 s) and by a factor of  $1.3 \times 10^6$  for a rare-isotope beam (the cooling period is equal to 1.5 s). The CR will also be used for mass measurements of short-lived nuclei.

- Recirculation Experimental Storage Ring (RESR), into which bunches of  $10^8$  antiprotons with an energy of 3 GeV stochastically cooled in the CR will be introduced every 10 s. This will enable accumulating up to  $10^{11}$  antiprotons in several hours to subsequently guide them to the HESR. The RESR will also provide a fast deceleration of rare isotopes, decreasing their energy from 740 to 100–500 MeV/nucleon in 1 s.

- New Experimental Storage Ring (NESR) intended for experiments with exotic ions and antiprotons. The NESR will employ both electron and stochastic cooling for experiments of different kinds, including those at very low energies (down to 30 MeV for antiprotons and to 4 MeV/nucleon for radioactive ion beams).

- High Energy Storage Ring (HESR), in which antiproton beams at energies up to 14.5 GeV will be prepared for experiments with the help of electron and stochastic cooling systems.

Extremely strict requirements concerning the quality of beams require the implementation of a highly sophisticated accelerator–storage FAIR scheme.

- Intensity problems. The technical requirements imposed on the fast-cycling magnets [7], in which the magnetic field will increase to 2 T at a rate of  $4 \text{ T s}^{-1}$  in the SIS-100 accelerator and to 6 T at a rate of  $1 \text{ T s}^{-1}$  in the SIS-300 accelerator, do not permit designers to confine themselves to presently existing technologies and make them direct their attention to technologies involving superconductivity with a record high field ramp rate.

- Induced radioactivity problems. Obtaining high-intensity particle beams will require developing materials of a new type and designing radiation-resistant accelerator and detector components capable of withstanding induced radioactivity.

- Acceleration problems. Fast acceleration of very heavy  $\text{U}^{28+}$  uranium ions requires complex radio-frequency devices generating extremely high-power high-frequency (RF) fields with steep edges and variable frequency, which are intended for the formation of short (50–100 ns) high-intensity particle bunches.

- Ultrahigh dynamic vacuum problems. The new materials and technical systems must sustain ultrahigh vacuum conditions ( $10^{-12}$  mbar) in the presence of high-intensity ion beams in the vacuum channels of accelerators and storage rings. Inevitable particle loss may give rise to desorption of molecules from the walls of devices, resulting in an unwanted increase in the residual gas pressure. Specially designed collimators are intended to minimize these effects. The more stringent ( $10^{-10}$ – $10^{-11}$  mbar) requirements (in comparison with those for the LHC) for vacuum conditions in the channels of the accelerator scheme stem from the necessity of accelerating ions with a wide mass and charge spectrum, including those having large capture and/or ionization cross sections for orbital electrons.

Russian participation in the construction of the accelerator complex is a logical continuation of the close long-term cooperation of Rosatom enterprises, the Russian Academy of Sciences, and the Ministry of Education and Science of the Russian Federation with the Institute for Heavy Ion Research (GSI), Darmstadt. Leading research institutes (the High-Energy Physics Institute, ITEP, JINR, the Budker Institute of Nuclear Physics (BINP) of the Siberian Branch of the RAS, the Joint Institute for High Temperatures of the RAS, the Institute for Chemical Physics Problems of the RAS, the Efremov Research Institute of Electrophysical Apparatus, the Troitsk Institute for Innovation and Fusion Research, the Bochvar All-Russia Research Institute of Inorganic Materials, etc.) are actively participating in the project development of the accelerator complex and in the preparation of experiments with ion and antiproton beams, as well as in the design and fabrication of new detectors.

### 3. Structure of atomic nucleus, astrophysics, and nuclear reactions with rare-isotope beams: NuSTAR experiment

Experiments relating to the area of NuSTAR (Nuclear STructure, Astrophysics, and Reactions) represent a broad spectrum of investigations in the physics of atomic nuclei, nuclear astrophysics, fundamental interactions, and symmetries.

Radically new aspects of nuclear structure manifest themselves in the investigation of exotic short-lived nuclei performed using secondary beams of radioactive nuclei [8–13]. Exotic nuclei are characterized by an extreme excess of protons or neutrons, and their states are therefore away from the valley of stability (Fig. 2). The structure of these nuclei would be expected to be substantially different from the structure of the nuclei corresponding to the valley of stability [14–16]. For instance, the proton and neutron density distributions in exotic nuclei, which are characterized by the presence of proton and neutron halos, are essentially different. Furthermore, such nuclei have excitation modes that do not exist in stable nuclei. The study of effects associated with exotic nuclei is of considerable importance in explaining the dependence of intranuclear forces, as well as of the pairing and clusterization effects, on the isotopic spin and density (see, e.g., Refs [17–20]).

Among the principal objectives of FAIR is the production of secondary beams of radioactive nuclei for the investigation of nuclear structure and the origin of elements in the Universe. According to modern views [21], there are more than 6000 different nuclei, the majority of them being unstable, especially those nuclei in which protons and neutrons differ significantly in number. Nuclei with complex and sometimes extraordinary structures may exhibit unusual behavior, which sheds light on the action of forces that prevent the nuclei from decaying.

Although some of these rare isotopes exist for only a very short time (less than  $10^{-6}$  s), they play a decisive role in nuclear reactions that produce heavy elements in stars. While light elements are formed during the life of stars in their thermonuclear burn, heavier elements (heavier than iron) are believed [2, 22, 23] to arise during the death agony of

supermassive stars, when the stars explode like supernovas. The explosion fragments then propagate through the interstellar space and finally become the building blocks for the next generation of stars and planets. The only way to verify these concepts is to produce and study unstable isotopes in laboratory. FAIR will produce the still unknown exotic nuclei and measure their masses, decay modes, and other properties, which is beyond the capabilities of any other laboratory in the world.

Therefore, with the rare-isotope beams of the FAIR accelerator complex, it will be possible for the first time to determine the properties of many unstable nuclei, like the lifetimes and decay channels and probabilities. These parameters are of considerable significance in elucidating the origin of heavy chemical elements and studying the physics of stellar explosions, nuclear processes in stars, and the properties of compact objects, in particular white dwarf, neutron, and peculiar stars [9]. New possibilities open up for studying the physics of thermonuclear explosions on the surface of giant stars, explaining the activity manifestation of new astrophysical effects, as well as the evolution of the Universe after the Big Bang.

Figure 2 shows the map of the intensities (in 1 s) expected of the FAIR radioactive beams for nuclei with lifetimes longer than 100 ns.

For research in this area, the new accelerator complex will provide secondary beams of radioactive nuclei throughout the charge and mass number ranges, from the lightest to the heaviest. These secondary beams of rare isotopes will be obtained either by fragmentation of the primary beams of heavy ions or by separation of  $^{238}\text{U}$  beams with energies up to 1.5 GeV/nucleon. The beams of nuclei with different charge and mass numbers will be separated using the new, partially superconducting magnetic Super Fragment Separator (Super-FRS) [24]. Its ion-optical diagram is shown in Fig. 3 in comparison with a similar diagram of the FRS separator at the GSI.

The beams of exotic nuclei are produced when a primary heavy-ion beam passes through a target. In this case, the ions split into other nuclei, which immediately undergo separation in a magnetic separator (Fig. 4). This permits obtaining high-purity beams of all kinds of isotopes (including short-lived ones) in a broad energy range and with temporal pulse characteristics matched to specific experiments. For the first time, the heaviest radioactive nuclei (up to uranium) will be produced in quantities sufficient for carrying out precision experiments (see Fig. 2).

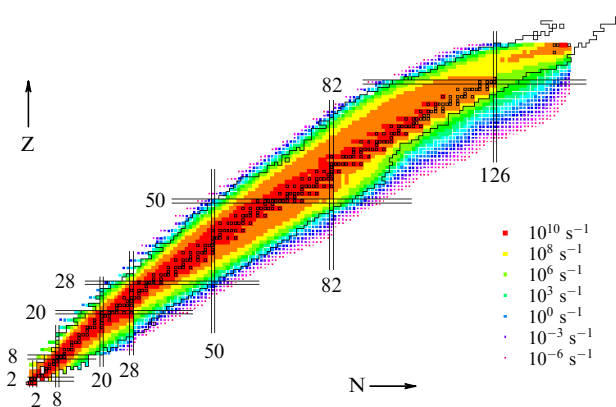


**Figure 2.** (Available in color online at [www.ufn.ru](http://www.ufn.ru)) Map of radioactive beam intensities in 1 s expected at FAIR (mapped in color in accordance with the scale column shown at the right of the figure). Parallel horizontal and vertical lines denote closed nuclear shells. The nuclei of primary beams and the boundaries of the domain of known nuclei are shown in black [4].

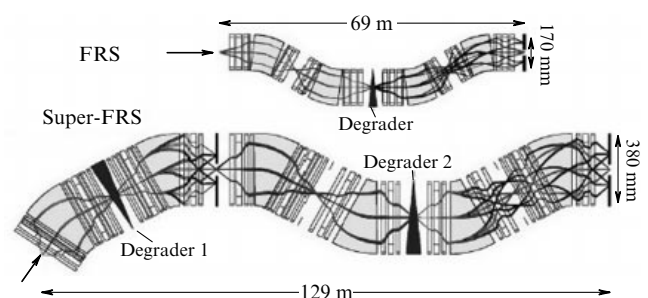


**Figure 3.** Comparison of the ion-optical diagrams of the new Super-FRS separator and the FRS separator at the GSI. For clarity, the longitudinal and transverse scales are made different, but equal for each of the separators [4].

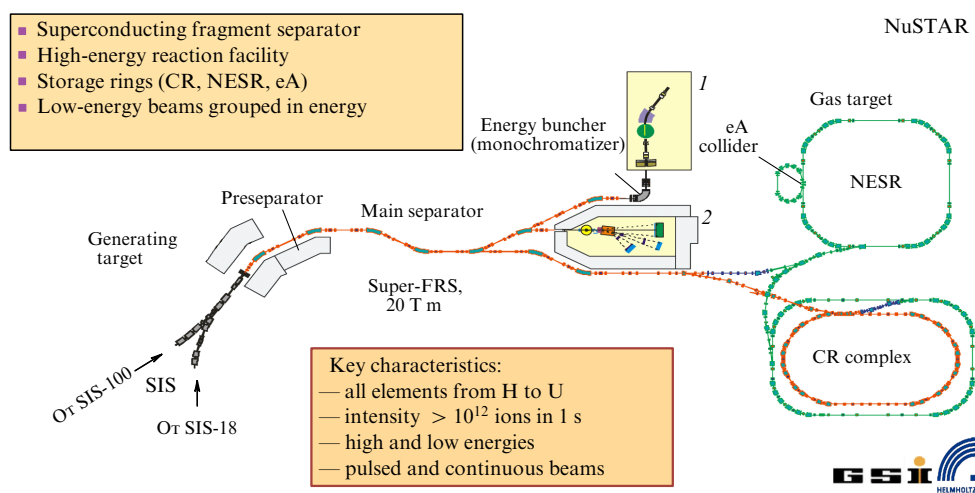


**Figure 4.** Schematic of NuSTAR experiments [4]. 1 — low-energy experimental chamber, 2 — high-energy experimental chamber.

The Super-FRS design incorporates the results of the operation of the GSI fragment separator, which relies on the principle of double magnetic analysis with intermediate selection in energy. The high intensity of the primary beams arriving from the SIS-100/300 causes the two-stage scheme of magnetic separators equipped with a wedge-shaped degrader (varied-thickness moderators), which permit monochromatizing the secondary beams [25] passing through due to the difference in particle energy loss in a variable-thickness substance.

The wide-aperture Super-FRS separator will have a high acceptance in momentum ( $\pm 2.5\%$ ) and angles ( $\pm 40$  mrad horizontal and  $\pm 20$  mrad vertical divergences) and an ion-optical resolving power of 1500. The new separator concept with two independent separation stages is used to handle the high loads and thereby efficiently suppress the background. About 30%–60% of the generated fission fragments will be extracted as spatially separated isotope beams.

The FAIR accelerators will be capable of producing the beams of even the shortest-lived isotopes and using them for research. Secondary beams will have a high degree of purity in a broad energy range while being endowed with a different temporal structure (pulsed or quasicontinuous). The secondary beams may be directed either to target stations or to storage rings.

Today, the NuSTAR research area encompasses eight experiments. The NuSTAR collaboration unites more than 800 participants from 37 countries. Russian participation in the experimental program in this area is represented by research groups from the National Research Center Kurchatov Institute, the Konstantinov St. Petersburg Institute of Nuclear Physics of the RAS, JINR, BINP, the Siberian Branch of the RAS, etc. The NuSTAR experimental programs are as follows:

- **Reactions with Relativistic Radioactive Beams (R<sup>3</sup>B):** investigation of the structure of atomic nuclei in nuclear reactions at high energies of radioactive ion beams. For this, universal, high-efficiency, high-resolution equipment having a large acceptance will be installed in the focal plane of the high-energy Super-FRS branch [25].

- **HIGH Resolution SPECTroscopy (HISPEC):** the use of intermediate-energy radioactive beams to investigate the evolution of the shell structure of highly neutron-excessive, medium-heavy nuclei using Coulomb excitation, knocking-

out, and secondary fragmentation reactions, as well as to study the evolution of the collective states of nuclei far away from the valley of stability (see Fig. 2) by measuring lifetimes and gyromagnetic ratios, i.e., the ratio of the dipole magnetic moment of an elementary particle (or a system of elementary particles) to its mechanical momentum.

- **DEcay SPECTroscopy (DESPEC):** the use of deep implantation of ions into an active stopper prior to their decay. A multisection detector will enable time and space correlation of the signal caused by the implantation of a heavy ion and the subsequent  $\beta$ -decay signal emerging in the detector itself. For exotic nuclei, investigations will be made of exotic decay modes like  $\beta$ -delayed neutron emission and fission or like direct neutron radioactivity. Studying the properties of the isomeric states of short-lived nuclei will be made possible.

- **Laser Spectroscopy of short-lived nuclei (LaSpec):** a study of stopped, cooled, and bunched radioactive ions [26–28] using a multipurpose laser spectroscopy facility under development, which together with the use of different optical methods will allow implementing a model-independent determination of the nuclear spins of isotopes and isomers, magnetic dipole moments, electric quadrupole moments, and root-mean-square variations of the radii.

- **Precision Measurement of very short-lived nuclei using an Advanced Trapping System for highly charged ions (MATS):** the MATS facility will be a unique combination of an Electron Beam Ion Trap (EBIT) intended for producing multiply charged ions, ion traps for beam preparation, and a high-precision system based on an electromagnetic Penning trap for measuring the masses (with a relative accuracy of about  $10^{-9}$ ) and studying the decays (conversion electrons and alpha particles) of radioactive nuclei. (See review [26] on precision nuclear physical measurements with the use of ion traps.)

- **Isomeric Beams, Lifetimes, and MAsses (ILIMA):** measurements of the masses and lifetimes of exotic nuclei in ground and isomeric states at relativistic energies. For this purpose, the ion beams of exotic nuclei will be injected into the CR storage ring. Measurements of the masses (correct to  $\pm 50$  keV) and lifetimes of very short-lived nuclei (to several microseconds) by way of measurement of the frequency spectra of the ions circulating in the storage ring (see, e.g., Ref. [29]) will be carried out in the CR operating in an



isochronous mode. Longer-lived nuclei (with lifetimes longer than 1 s), after their preliminary stochastic cooling in the CR, will be directed to the next ring, the RESR, and then injected into the NESR. Here, the nuclei will undergo additional electron cooling, after which their masses will be measured by a similar method [30]. Additional transferable particle identification detectors will be installed behind one of the dipole magnets in the CR and the NESR for independent lifetime measurements.

- **EXotic nuclei studied in Light-ion induced reactions in the NESR (EXL):** a study of direct reactions of exotic nuclei with light stable nuclei in inverse kinematics with the aid of modern storage accelerator techniques and a universal detector system. Earlier investigations with stable nuclei showed clearly that such direct reactions involving light nuclei at intermediate and high energies are the necessary tool for studying the structure of atomic nuclei. The EXL detector system installed at the NESR will comprise:

- (1) a nuclear recoil silicon detector of reaction products, which is located around the inner gas-jet target; the detector is supplemented with slow-neutron detectors and a highly segmented scintillator assembly for recording  $\gamma$ -ray photons and measuring the total energy of higher-energy target recoil nuclei;

- (2) detectors for forward outgoing fast neutrons and light charged particles;

- (3) detectors for heavy fragments ejected from the gas-jet target.

- **ELectron–Ion Scattering experiment in the NESR (ELISe):** a study of the structure of exotic nuclei in experiments on elastic, inelastic, and quasi-free electron scattering from ions using the intersecting ion (NESR) and electron (ER) storage rings and an electron spectrometer operating in combination with a system for detecting reaction products. The most reliable data on the density distribution in atomic nuclei were obtained precisely from electron scattering experiments. Until presently, however, experiments on electron scattering from nuclei have been limited to stable isotopes. The objective of the ELISe program is to develop this powerful tool, which has already yielded a wealth of valuable information about the structure of stable nuclei, and extend its applicability to nuclear states that are far from the stability domain. For this, secondary beams of radioactive ions cooled in the NESR will be collided with a high-intensity electron beam that circulates in the electron storage ring intersecting with the NESR.

The secondary beams (see Fig. 4) are distributed for the execution of experiments in three directions:

- a high-energy branch: an investigation of astrophysically important reactions with high-energy heavy ions for inverse kinematics using the highest-efficiency detection and coverage of the total solid angle—the R<sup>3</sup>B experiment (in which heavy particles in the beam interact with light target nuclei and secondary particles are detected at large angles);

- a low-energy branch: a study of nuclei properties like decay modes and energy levels with the use of monoenergetic low-energy (from a few to 100 MeV per nucleon) ion beams—HISPEC, MATS, LaSpec, and DESPEC experiments;

- a branch directed to the CR–RESR–NESR ring system, in which exotic nuclei are stored, cooled, and accumulated, for experiments on mass and lifetime measurements for unknown exotic nuclei, as well as in the study of their structure with the help of electron or antiproton beams—ILIMA, EXL, and ELISe experiments.

In many respects, the experiments developed at FAIR will significantly excel in capability experiments with radioactive nuclear beams at other scientific centers. FAIR will offer significant advantages in comparison with similar projects in the USA (RIA (Rare Isotope Accelerator) at the Argonne National Laboratory [31] and LEBIT (Low Energy Beam and Ion Trap) at Michigan State University [32]), Europe (REX-ISOLDE (Radioactive beam EXperiment at ISOLDE) at CERN [33], SPIRAL-2 (Système de Production d'Ions Radioactifs Accélérés en Ligne) at the Ganil Research Center [34], CYCLONE (CYClotron of LOuvain-la-NEuve) [35] at Louvain-la-Neuve University, MAFF (Munich Accelerator for Fission Fragments) at Ludwig-Maximilian-University, Munich [36], SHIP (Separator for Heavy Ion reaction Products) [37] and SHIPTRAP [28] at the GSI), and Japan (RIBF (Radio-Isotope Beam Factory) [37] at the RIKEN Research Center) owing to the application of new technologies, the high intensities of secondary radioactive beams, which are highest in intensity—up to 1.5 GeV/nucleon (for comparison: 400 MeV/nucleon in the RIA and 350 MeV/nucleon in the RIBF)—over a wide mass range, and primarily owing to the unique combination of the Super-FRS wide-aperture fragment separator and the CR–RESR–NESR system of storage rings [38].

## 4. Dense baryon matter: the CBM experiment

### 4.1 CBM scientific program

The scientific program of the CBM (Compressed Baryonic Matter) experiment comprises investigations of extreme nuclear matter states and the phase transition to the quark–gluon plasma at a high baryon density in nuclear–nuclear collisions; investigations of the structure and equation of state of baryon matter at densities comparable to the core density of neutron and quark–gluon ('strange') stars [2]; a search for the boundary between the baryon and quark–gluon matter phases; the quest for the critical point and indications of the onset of chiral symmetry restoration at high baryon density (Fig. 5) [39]; and many others.

The energy of heavy ions on FAIR's SIS-300 will amount to 35–45 GeV/nucleon for an intensity 1000 times higher than the present-day intensity of the SIS-18 accelerator at the GSI and a 10 times higher than the LHC beam intensity [40]. The projected research will allow a substantial advancement in the

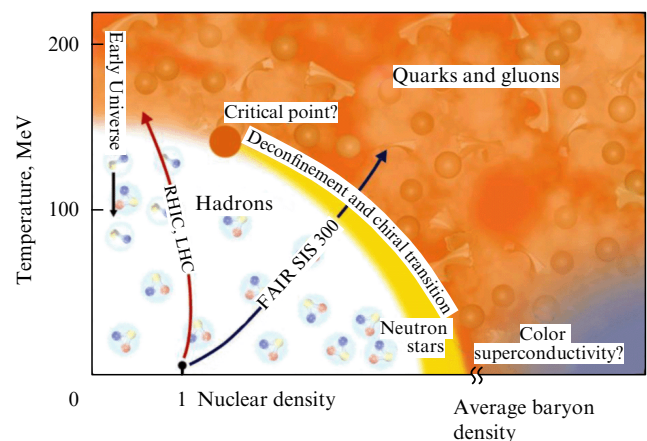


Figure 5. Phase diagram of nuclear matter.

investigation of unknown phase diagram domains over experiments on the RHIC and the LHC [41], in which the emphasis is on the investigation of the properties of matter at extremely high temperatures and low baryon densities, i.e., at very low values of the baryon chemical potential. By contrast, the FAIR CBM experiment is aimed at a detailed study of those properties at the highest baryon densities that can be attained under terrestrial conditions (Fig. 5).

To explore the behavior of nuclear matter at the high densities typical for supernova explosions and compact astrophysical objects, experiments will be executed at FAIR involving collisions of heavy ions with fixed targets at energies providing maximal nuclear matter compression. It is hypothesized that the protons and neutrons of atomic nuclei ‘dissolve’ into a quark–gluon plasma at extremely high densities. This phase transition to a new state, which lasts for only  $10^{-23}$  s, should be observable in central collisions between nuclei at the high energies attainable on FAIR’s SIS-300 accelerator [42].

Unlike experiments at CERN and the Brookhaven National Laboratory, where the search for the critical point is carried out only by recording the spectral characteristics of secondary particle fluxes (the bulk observables), owing to a high intensity of primary beams, the FAIR experiments open up an additional possibility of detecting rare events with the scanning of a vast domain of the phase diagram in particle energies. In particular, for the first time it is planned to directly investigate the signatures of the emergence of a fireball—the domain of nuclear matter in which the baryon-to-quark–gluon phase transition occurred—by detecting short-lived vector mesons that decay to electron–positron (dilepton) pairs.

The 2–35 GeV/nucleon FAIR energy range for gold ions is well suited to the execution of experiments in the phase diagram area with high nuclear matter densities exceeding the normal density by a factor of 8–10.

Of importance for unambiguous data interpretation is the opportunity to make a direct comparison of the data obtained in nucleus–nucleus collisions with the data of proton–proton and proton–nucleus collisions, because the FAIR accelerator complex will generate proton beams with energies up to 90 GeV.

#### 4.2 CBM detector

The detector being developed by the CBM collaboration is schematized in Fig. 6 [43]. The universal detection system will identify particles produced in the dense reaction zone. Experiments will run with  $10^7$  events per second and up to 1000 charged particles will be detected per central collision of gold ions [40].

A radiation-resistant silicon track recorder—STS (Silicon Tracking System)—consists of three planar layers of silicon pixel and strip detectors followed by four layers of microstrip detectors. The entire detector is located in the gap of a dipole magnet for determining the momentum with a resolution better than 1%. The function of a Ring Imaging CHerenkov detector (RICH) consists in the identification of electrons and the suppression of pions in the momentum range of the electrons arising from the decay of low-energy vector mesons. A Transition Radiation Detector (TRD) will provide charged particle tracking and identification of fast electrons and positrons. The challenge is to develop highly granulated detectors (gas counters) capable of operating at rates up to  $100 \text{ kHz cm}^{-2}$ . At the same time, the pion

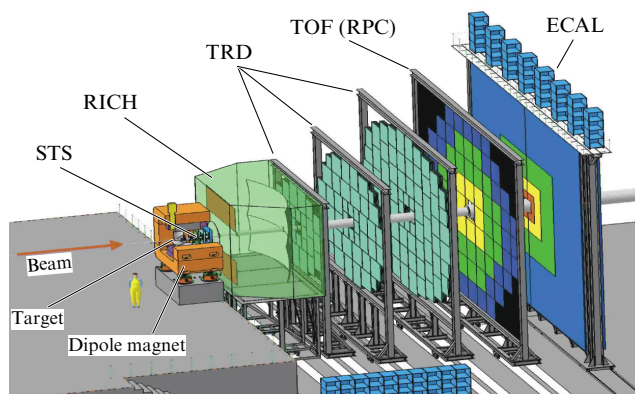


**Figure 6.** CBM detector (see text for explanations and interpretation of abbreviations).

discrimination factor must be as high as several hundred for an electron detection efficiency of 90%. Hadrons will be identified with a time-of-flight (TOF) system based on resistive plate chambers (RPC). The admissible error of measurements should not exceed 100 ps for particle fluxes up to  $25 \text{ kHz cm}^{-2}$ . An Electromagnetic CALorimeter (ECAL), made with the unique Russian technology termed ‘shashlyk’ (shish kebab; see, e.g., Refs [43–45]), will be used to identify electrons and photons and to reject pions.

### 5. Antiproton annihilation: the PANDA experiment

#### 5.1 Physics program with antiproton beams

The physics program of the PANDA (anti-Proton ANnihilation in DArmstadt) experiment covers a broad research area: from investigations into the basic hadronic and nuclear physics problems to verification of fundamental symmetries by studying the interaction of accelerated antiprotons with nucleons and atomic nuclei with the use of a universal PANDA detector mounted on the axis of the HESR high-energy storage accelerator (Fig. 7).

The physical program is aimed at searching for new forms of matter; in this case, an unprecedentedly high accuracy will be reached in the investigation of gluon excitations and in the physics of strange and charmed quarks [4, 46], which is provided by two fundamental features of the FAIR accelerator complex: (a) the availability of a high-intensity antiproton beam with the energy up to 15 GeV, and (b) the capability of fine scanning of the antiproton energy with an accuracy of  $\pm 10 \text{ keV}$ . This permits executing the experimental investigations of strong interaction properties at a new level of precision.

Experimental investigations into the structure of both ordinary and exotic hadrons may be carried out using electron, pion, kaon, proton, or antiproton beams. In the course of hadron annihilation, in particular antiproton–nucleon and antiproton–nucleus ones, particles with gluon degrees of freedom, like particle–antiparticle pairs, are produced in abundance. This permits carrying out spectroscopic investigations with an extraordinarily large statistics and high accuracy. Therefore, the antiproton beams of the FAIR accelerator complex—in combination with the PANDA detector—will allow the acquisition of qualitatively new results in comparison with the results of experi-



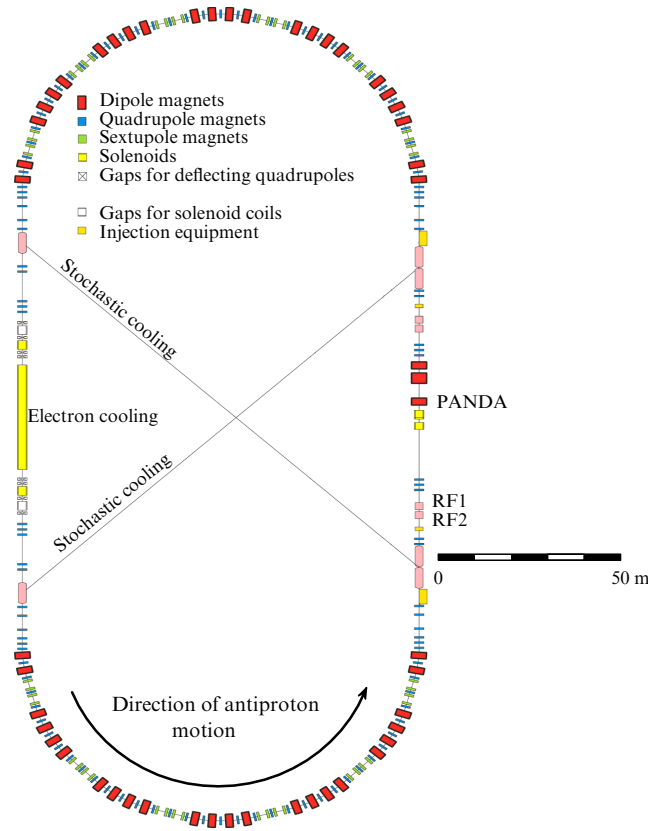


**Figure 7.** HESR antiproton storage accelerator with the PANDA detector [4].

ments performed at the Fermi National Laboratory (Fermilab, USA) and at CERN. FAIR will provide a 100-times-higher intensity of stored and cooled antiprotons than at CERN and will also exceed in intensity the beams at the Fermilab and the J-Park facility being constructed in Japan [4, 47].

For the first time, high-precision measurements will become possible not only for electromagnetic but also for hadronic decay modes in resonance proton–antiproton annihilation, as will the quest for gluon excitations (glueballs and hybrids) in the energy range corresponding to the charmonium masses 3–5 GeV/ $c^2$  (Fig. 8).

The unambiguous determination of gluon modes will be an important step in solving the problem of quark confinement in hadrons. In particular, a particle consisting of a charmed quark and an antiquark (charmonium) will allow high-accuracy studies of the heretofore unexplored aspects of the strong interaction, whose main theory now is QCD. The PANDA experiment will open up broad possibilities for discoveries, in addition to experiments on the LHC for a relatively high antiproton energy; furthermore, owing to energy scanning with an accuracy of 10 keV, it will allow determining the widths of narrow resonances, like the states of charmonium.

The PANDA scientific collaboration program comprises:

- the quest for exotic particles, like glueballs and hybrids;
- the spectroscopy of charmonium states at energies exceeding the energy threshold of D–anti-D-meson pair production;
- investigations of hypernuclei (including double ones) and charmed nuclei, in which strange (one or two) or charmed particles replace an ordinary nucleon.

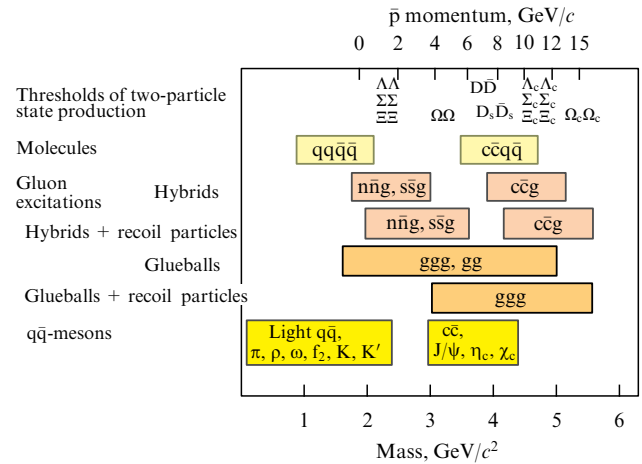


**Figure 8.** Hadronic mass range that will be available in PANDA experiments. The upper scale shows the corresponding antiproton momenta required for fixed-target experiments [4].

Also projected is the use of the PANDA facility for studying rare decays that contain single photons,  $\pi^0$  and  $\eta$  mesons in a broad energy range (see Fig. 8).

It is expected that the PANDA experiments will be carried out in two modes: a high-luminosity mode and a high-resolution mode. The high resolution in momentum is achieved by beam cooling, whose efficiency decreases with intensity because of intrabeam scattering. The parameters characterizing these modes are collected in Table 2.

The protons accelerated in SIS-100 to the energy of 29 GeV are employed to generate a beam of antiprotons, which are produced under bombardment of a thin target by protons, subsequently cooled in two rings (CR and RESR), and delivered to the HESR, schematized in Fig. 7. In the HESR, the antiproton beams interact with an internal thin proton target (hydrogen) to produce composite particles containing strange and charmed quarks.

Two types of internal hydrogen-beam targets will be used in the PANDA experiments: a cluster jet target (see, e.g., Refs [48, 49]), in which the clusters are particles consisting of about  $10^5$  weakly coupled hydrogen atoms, and a target represented by a train of frozen hydrogen microspheres falling in a vacuum [50], so-called pellets with characteristic diameters of 20–40  $\mu\text{m}$ .

Similar targets of other gases (for instance, neon, nitrogen, argon, xenon) will also be available for the PANDA experiments.

**Table 2.** Parameters of PANDA's two experimental modes (assuming that the effective thickness of the internal hydrogen target is  $4 \times 10^{15}$  atoms per  $1 \text{ cm}^2$  and the beam emittance is 0.3 mm mrad).

Parameter	Operating mode	
	High resolution	High intensity
Momentum range, GeV/ $c$	1.5–8.9	1.5–15
Number of stored antiprotons	$1 \times 10^{10}$	$1 \times 10^{11}$
Beam luminosity, $\text{cm}^{-2} \text{ s}^{-1}$	$2 \times 10^{31}$	$2 \times 10^{32}$
Momentum resolution $\delta p/p$	$< 4 \times 10^{-5}$	$1 \times 10^{-4}$

Antiproton beams for the PANDA experiments will be obtained as follows [7]. Initially, 40- $\mu$ s-long proton bunches with the current of 70 mA and the pulse repetition rate of 5 Hz accelerated to an energy of 70 MeV in the p-LINAC linear accelerator will be injected into the SIS-18 synchrotron.

To increase the number of accelerated protons, the ring of the SIS-18 synchrotron will be filled with eight sequential proton bunches prior to their acceleration to the energy of 2 GeV required for the subsequent injection into the main FAIR accelerator, the SIS-100 synchrotron.

In SIS-100, the protons will be accelerated to their final energy of 29 GeV and, prior to their extraction to an antiproton producing target, will be compressed to one bunch approximately 7.5 m in length, which corresponds to a duration of  $\approx 25$  ns. Every 10 s, the bunch of  $2 \times 10^{13}$  protons will be extracted onto a thick iridium or tungsten target (with the effective thickness 60–80 mm), producing  $1 \times 10^8$  antiprotons (with a yield of  $5 \times 10^{-6}$  per proton) with an average energy of 3 GeV.

A magnetic system is employed to ‘cut out’ a short bunch of antiprotons with a momentum spread  $\delta p/p = \pm 3\%$  and a transverse emittance  $\varepsilon_{x,y} = 200$  mm mrad from the resultant spectrum (the process efficiency is  $\approx 2$ –3%). Then the beam is injected into the CR storage ring, where its phase volume is transformed such that the bunch lengthens from  $l_b \approx 15$  m to  $l_b \approx 45$  m, with a corresponding decrease in the momentum spread to  $\delta p/p = \pm 1\%$ . Subsequently, due to free circulation in the ring, the beam loses its pulsed structure (so-called adiabatic rebunching) and is thereby prepared for cooling. On stochastic cooling, the antiproton beam ( $\delta p/p = \pm 0.1\%$ ,  $\varepsilon_{x,y} = 5\pi$  mm mrad) is grouped into bunches once again and delivered to the RESR, where antiprotons are accumulated.

In the RESR, the antiproton beam undergoes stochastic cooling throughout the accumulation period during which a new antiproton bunch is injected into the RESR every 10 s. The antiproton accumulation rate is comparable to the antiproton cooling rate in the CR. This signifies that up to  $7 \times 10^{10}$  antiprotons can be produced in 1 h. The choice of the accumulation period (or the total number of stored antiprotons) is determined by experiment requirements.

Before the antiprotons stored in the RESR are injected into the HESR, the antiproton beam with a momentum of 3.8 GeV/c is compressed into one bunch. In the HESR, at a rate of about 0.1 GeV/c, the antiproton beam may be either accelerated or decelerated to the momentum required in a given experiment.

Thus, the FAIR accelerator complex will provide antiproton beams with unprecedentedly high intensities and quality in the momentum range from 1.5 to 15 GeV/c (or the energy range from 0.83 to 14.1 GeV) for annihilation experiments using an internal target and the universal 4 $\pi$  PANDA detector. Up to  $\sim 10^{11}$  antiprotons may circulate in its 574-m-long ring. To compensate for the negative effect of the antiproton beam heating arising from its interaction with the internal target and intrabeam scattering, the HESR will be equipped with an electron cooling facility with an electron energy up to 4.5 MeV and a system of stochastic cooling.

## 5.2 PANDA detector

PANDA is a 4 $\pi$  detector with an internal fixed target and is installed in the HESR.

The PANDA detector, with the acceptance close to 4 $\pi$ , high resolution in tracking, particle identification, and

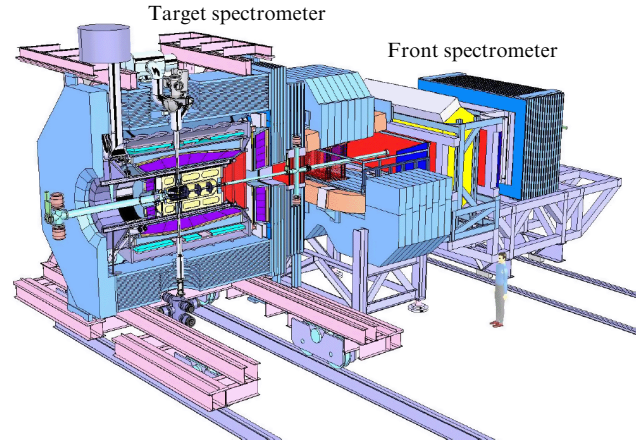


**Figure 9.** PANDA detector, which consists of two magnetic spectrometers: the target spectrometer arranged around the antiproton–target interaction point and the front spectrometer intended for measuring the tracks of particles emanating from the target at low angles to the antiproton beam axis. The overall detector length is 10 m [4].

calorimetry, will provide efficient data collection and selection of events for the rate of  $2 \times 10^7$  interactions per second in the inner hydrogen target [46].

To provide a high momentum resolution, the detector will consist of two magnetic spectrometers (Fig. 9): the target spectrometer based on a superconducting magnetic solenoid, which is arranged around the antiproton–target interaction point and will be used for measurements at large angles, and the front spectrometer, which has a dipole magnet for measuring the tracks of particles emanating from the target at small angles to the antiproton beam axis.

Both spectrometers will afford tracking, charged particle identification, electromagnetic calorimetry, and muon identification, which will permit recording the entire spectrum of the final states important for achieving the goals of the PANDA research collaboration program.

The target spectrometer, which is schematically shown in Fig. 10, will measure the tracks of charged particles in a highly uniform (to within  $\pm 2\%$ ), 2 T solenoidal field. The spectrometer configuration (similar to the configuration of detectors in collider experiments) is like the structure of an onion: different types of detectors will be arranged in layers about the axis. Vacuum pipes intended for the introduction and subsequent removal of the target material (i.e., a beam of clusters or pellets) from the antiproton beam will cross the spectrometer vertically, perpendicular to the vacuum pipe with the antiproton beam. In accordance with the angles of particle escape from the target, this spectrometer may be conventionally divided into the following three parts: the barrel, which covers the angular range between  $22^\circ$  and  $140^\circ$ , the front end cup, which broadens the angular range to the lower side to  $5^\circ$  in the vertical plane and to  $10^\circ$  horizontally, and the rear end cup, which covers the  $\approx 145^\circ$ – $170^\circ$  angular range.

We briefly describe the key elements of the target spectrometer.

A superconducting solenoid. Providing a 2 T magnetic field in a 4-m long space of diameter 1.9 m available for detector installation is a nontrivial technical problem, which is additionally complicated by the strict requirements imposed on the uniformity of magnetic field, the presence of magnet-intersecting hot pipes for target beam transport, the

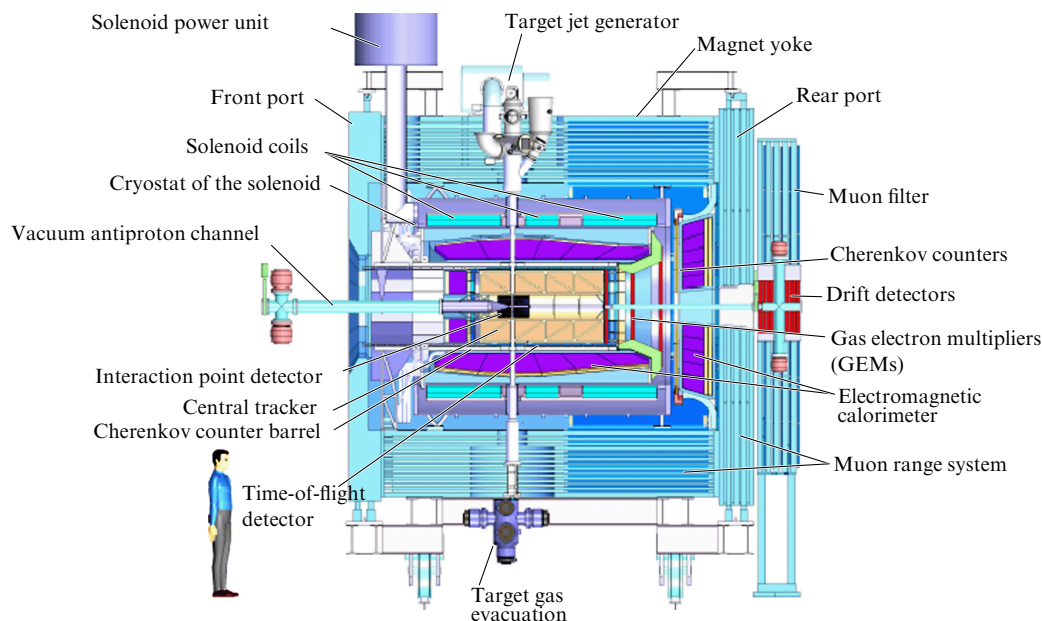


**Figure 10.** Side view of the target spectrometer of the PANDA detector.

need to provide access to detectors, etc. The cryostat of the solenoid will surround all detectors and serve as their support structure. The magnet yoke will additionally play the role of a muon detection system, due to the placement of minidrift tubes in it (between 13 iron layers)—the Muon Range System (see Fig. 10). The main parameters of the superconducting solenoid are collected in Table 3.

A micro-vertex detector is located in the target spectrometer, closest to the point of interaction of the antiproton beam with the transverse beam of target particles. The micro-vertex detector, whose concept relies on the use of radiation-resistant silicon pixel and strip detectors, is a tracking device for charged particles. This detector is highly important for the precise determination of the vertices of secondary decays of short-lived particles, like charmed or strange hyperons and D mesons.

A central tracker is arranged around the micro-vertex detector and is the central track detector, which is also barrel-shaped; its operation is based on the ionization of gas in the passage of a charged particle through it. The electrons resulting from the ionization drift to the sensor electrode in the field applied, and the charged particle track can be determined from the known drift velocity in the gas and the spatial position of the electrode.

At present, the following two detector systems are considered as versions for the central tracker realization.

The first system (straw tube tracker) is a multilayer assembly of 4200 self-sustained drift tubes with walls made of thin (30  $\mu\text{m}$ ) aluminized mylar film, which have a gold-coated tungsten or rhenium electrode 20  $\mu\text{m}$  in diameter on their axis. The length and diameter of the tubes are respectively equal to 150 cm and 10 mm. The tubes are filled with a mixture of argon (90%) and carbon dioxide (10%).

The second system (time projection chamber) consists of two large gas-filled semicylindrical chambers, whose end faces (lids) play the role of electrodes (cathode and anode). The electric field aligned with the cylinder axis makes the electrons produced by charged particles passing through the gas move steadily toward the anode, which is designed in the

**Table 3.** Main parameters of the superconducting solenoid.

Central field	2.0 T
Field nonuniformity	$\leq 2\%$
Inner diameter	1.9 m
Cold mass parameters	
Length	2.7 m
Energy	20 MJ
Current	5000 A
Weight	4.5 t
Cable section	$3.4 \times 2$ mm
Current density	$59 \text{ A mm}^{-2}$
Yoke parameters	
Length	4.9 m
Outer diameter	4.6 m
Number of iron layers	13
Total weight	300 t

form of a matrix of separate small-size sensors. It is thus possible to obtain information about two coordinates of a track, and its third coordinate is determined from measurements of the drift time of electrons from the point of their initial production in the gas to the anode, where they are detected.

Gas electron multipliers (GEMs). Particles traveling at angles  $< 22^\circ$  to the axis, i.e., particles that do not enter the central tracker, will be detected by three gas electron multiplier stations mounted at distances of 1.17, 1.53, and 1.89 m from the target.

Particle identifiers. The capability of identifying hadrons and leptons in a broad range of momenta and angles is an



important property of the PANDA facility. Particles with momenta greater than 1 GeV/c will be identified by Cherenkov detectors. Slow particles ejected at large angles will be identified by a time-of-flight detector. Because the target spectrometer path length is only 50–100 cm, this detector must have a very good temporal resolution, about 50–100 ps. The time-of-flight detector assembly in the form of a barrel (Barrel TOF) with inner and outer radii 42 and 45 cm will cover angles between  $22^\circ$  and  $140^\circ$ . Faster particles in this angular range will be identified by detection of internally reflected Cherenkov (DIRC) light, as was realized in the BaBar facility [51]. The Cherenkov detector will be a barrel-like assembly (Barrel DIRC) of quartz plates 1.7 cm in thickness surrounding the antiproton beam at a distance of 45–54 cm from the axis. A similar Cherenkov detector, although in the form of a disc (Disc DIRC), will be used for particles ejected forward at angles between  $5^\circ$  and  $22^\circ$ . This disc will be mounted immediately in front of the front end cup of the electromagnetic calorimeter.

**Electromagnetic calorimeter.** To operate at a high rate of events, the electromagnetic calorimeter needs a fast scintillation material with a short radiation length  $X_0$ . Best suited for this purpose are crystals of lead tungstate ( $\text{PbWO}_4$ )—a high-density inorganic material that provides a high energy and time resolution in the detection of photons and electrons, even in the intermediate energy range [52]. This is precisely the reason why  $\text{PbWO}_4$  crystals are used, for instance, in the compact muon spectrometer of the Compact Muon Solenoid (CMS) collaboration at CERN [53]. To reach the energy resolution better than 2% at an energy of 1 GeV, the crystals in the electromagnetic calorimeter must be of 20 cm in length (i.e., approximately  $22 X_0$ ). 11,360 profiled crystals with a front face area of  $2.1 \times 2.1 \text{ cm}^2$  will be installed in the calorimeter barrel with an inner radius of 57 cm. The front and rear end cups of the barrel will respectively require 3600 and 592 crystals. Therefore, the total number of  $\text{PbWO}_4$  crystals will be equal to 15,552. The main design parameters of the electromagnetic calorimeter are collected in Table 4.

The front spectrometer (Fig. 11) will record particles emitted in the respective vertical and horizontal angular ranges of  $\pm 5^\circ$  and  $\pm 10^\circ$ . To analyze the charged particles with a momentum resolution of  $\leq 1\%$ , a dipole magnet with a gap of 1 m and an aperture of 2 m will be used. The deflecting force of the magnet is equal to 2 T m, which makes antiprotons with the maximum momentum equal to 15 GeV/c deflect by an angle of  $2.3^\circ$  in its field. The antiproton beam deflection will then be compensated by two or three beam-positioning magnets installed behind the PANDA facility.

**Table 4.** Main design parameters of the electromagnetic calorimeter.

Material	$\text{PbWO}_4$
Crystal dimensions	$2 \text{ cm} \times 2 \text{ cm} \times 20 \text{ cm}$
Length	$22 X_0$
Energy resolution	$1.54 \% / \sqrt{E [\text{GeV}]} + 0.3 \%$
Time resolution	$< 20 \text{ ns}$
Number of crystals	15,552
Solid angle covered	$96 \% 4\pi$

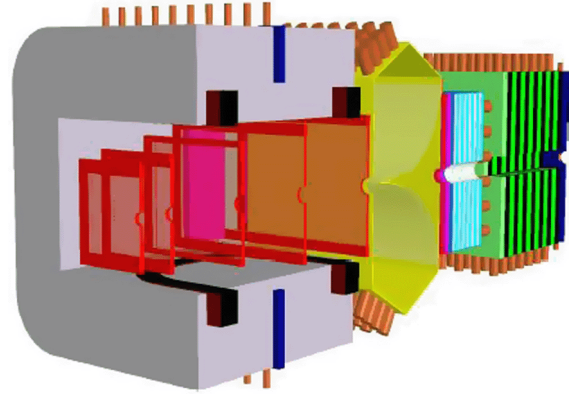


**Figure 11.** Three-dimensional structural view of the front spectrometer of the PANDA detector. The dipole magnet (at the left of the figure) with a 1-m gap and an aperture greater than 2 m possesses a deflecting force of 2 T m.

The variations of particle trajectories in the field of the dipole magnet will be measured by multiwire drift chambers. Two chambers will be installed in front of the magnet and two more behind the magnet. This will enable recording the tracks of the highest-momentum particles. Two additional drift chambers will be installed inside the magnet gap for tracking particles with small momenta.

An assembly of plastic scintillator plates with fast photomultipliers at both ends of the plates for signal read-out, placed at a distance of 7 m from the target, will serve as stop time-of-flight counters for measuring the transit time from the start detector, which is placed near the target, to these stop counters. Similar stop detectors will be additionally installed inside the dipole magnet for detecting low-energy particles that cannot escape from this magnet. For an expected time resolution of 50 ps, separation of pions from kaons ( $\pi/K$ ) and of kaons from protons ( $K/p$ ) at the level of three standard errors will be possible for particles with respective momenta up to 2.8 and 4.7 GeV/c.

The calorimeter for particles ejected into the front angular domain will consist of two parts. A shashlyk calorimeter (see, e.g., Ref. [44]) will be used in the first part intended for detecting photons and electrons with high resolution and efficiency. An energy resolution of  $4\%/\sqrt{E}$  was derived for this calorimeter type in Ref. [54]. The second calorimeter part will fulfill the function of measuring the energies of neutral hadrons and will also be used as a fast trigger and an active muon filter. This calorimeter part will be installed immediately behind the calorimeter, in front of the wall of muon identification counters (these counters are similar to the muon counters that surround the superconducting solenoid of the target spectrometer described above). A comprehensive description of the front spectrometer can be found in Ref. [55].

## 6. Physics of high energy density in matter: plasma physics

Research in the physics of high energy density in matter and extreme states of matter exposed to high-intensity pulsed action is necessary for acquiring new knowledge about the physical processes and material properties under conditions of superhigh pressure, density, and temperature. This knowledge forms the scientific basis for challenging energy projects: controlled nuclear fusion (CNF) with inertial confinement of

hot plasma, magnetohydrodynamic and magnetocumulative generators, nuclear space facilities, etc. [2]. Furthermore, this knowledge is used for improving the properties of materials of nuclear power facilities experiencing the action of high-power radiation fluxes and for developing new energy application technologies.

Proceeding from experimental data, highly reliable mathematical physics models are being developed that have strong prognostic capacities and will underlie computer simulations. The accuracy of predictions of such simulations relies on the basic models used, the depth of understanding the essence of the physical processes involved, and the reliability of the description of material properties under ultrahigh pressures and temperatures.

Record high pressures of matter in the range of densities  $1\text{--}1000\text{ g cm}^{-3}$  and temperatures  $10^{-1}\text{--}10^5\text{ eV}$  were earlier obtained in underground nuclear tests [2]. At present, the possibility has arisen to obtain experimental data on research facilities that permit covering one domain or another of the phase diagram of matter. The largest of them are Omega and NIF (National Ignition Facility) (USA), Gekko-12 (Japan), Vulkan (Great Britain), and Iskra-5 (Russia) high-power lasers, ZX (USA) and Angara-5-1 (Russia) high-power electric discharge systems, and SIS-18 (Germany) and TWAC-ITEP (Russia) high-power heavy-ion accelerators. Figure 12 shows the capabilities of various facilities for research in different domains of the phase diagram of matter.

At the FAIR complex, it will be possible to achieve a pulsed ion-beam intensity  $\sim 10^{12}$  for an energy up to 1000 MeV/nucleon. By increasing the intensity of heavy (up to uranium) ion beams and compressing the beams in time to a pulse duration of 50 ns, the specific energy input of the FAIR facility will be made 600(!) times higher than that of the SIS-18 accelerator complex at the Heavy Ion Institute and 10 times higher than that of TWAC-ITEP, which is under construction at Rosatom. This will enable studying the properties of superdense nonideal plasmas and of matter under ultrahigh pressure, which is required for developing the technologies of inertial confinement fusion and simulating

nuclear explosions at unprecedentedly high levels of statistical accuracy in density and temperature ranges unattainable with other experimental facilities.

Two major international collaborations, HEDgeHOB (High Energy Density generated by Heavy Ion Beams) and WDM, serve the purpose of using the property of volumetric energy release by a high-intensity ion beam in matter to generate states of matter with a high level of entropy. The high-power pulsed beams that will be generated by the FAIR accelerators are capable of producing large volumes of dense plasma with an energy density that is of interest for the solution of a broad range of fundamental problems in plasma physics, radiative hydrodynamics and magnetohydrodynamics, the radiative study of materials, planetary geophysics, atomic and molecular physics, etc. The expected parameters of  $\text{U}^{28+}$  ion beams are collected in Table 5.

On focusing to a spot  $\approx 1\text{ mm}$  in diameter, ion beams with the above parameters are able to heat macroscopic volumes of a dense target substance to a temperature of several dozen electronvolts.

The heart of the experimental research program on the physics of high energy density in matter comprises three basic experiments:

- Heavy Ion Heating and EXpansion (HIHEX);
- Laboratory PLANetary Science (LAPLAS);
- Warm Dense Matter (WDM).

The most important feature of these three experiments on the FAIR accelerators will consist in the unique possibility of plasma diagnostics using high-energy proton beams (radiography) with the simultaneous use of high-power petawatt laser radiation ( $\approx 10^{15}\text{ W}$ ). This laser is capable of producing a target irradiation intensity of  $10^{21}\text{ W cm}^{-2}$ . Planned under the program is the construction of a corresponding proton beam transport line from the SIS-18 accelerator to the experimental plasma physics chamber, as well as of a transport line for the delivery of high-power laser radiation to the target vacuum chambers. The combination of the high-intensity laser pulse, the diagnostic proton beam, and the high-intensity ion beam opens up new, unique experimental possibilities for FAIR.

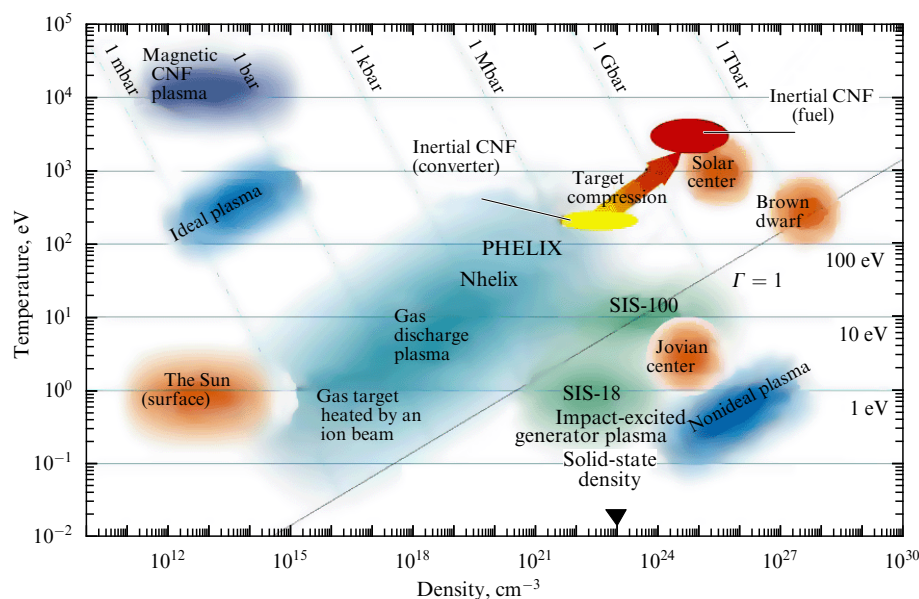


Figure 12. Phase diagram of matter. (Nhelix is a nanosecond high energy laser for ion beam experiments at the GSI).



**Table 5.** Parameters of  $U^{28+}$  ion beams.

Parameter	Value
Total pulse energy	80 kJ
Pulse duration	50 ns
Total number of particles	$2 \times 10^{12}$
Specific power	10 TW g <sup>-1</sup>
Specific energy liberation	> 100 kJ g <sup>-1</sup>
Ion energy	~ 1 GeV/nucleon

### 6.1 HIHEX experiment

High-intensity heavy-ion beams with a pulse duration of 50–100 ns make it possible to rapidly (in comparison with the characteristic time of hydrodynamic motion) heat a substance and then observe the expansion of the hot substance in the surrounding medium, i.e., create a high level of energy deposition and successively observe the isentropic expansion. In an experiment of this type [1, 56], the heated material goes through several new interesting states in its expansion. Specifically, as a result of heating, an initial metal of normal density reaches the superheated liquid state with a disordered ion component and degenerate electrons. During isentropic expansion, the substance goes through the state of a quasi-nonideal Boltzmann plasma and a rarefied gas. On further expansion, the degree of degeneracy decreases, which is attended by a redistribution of the energy spectrum of ions and atoms, as well as a partial recombination of dense plasma. Metal–dielectric phase transitions can occur in a disordered electron system, and the plasma in the vicinities of the critical point and the liquid–vapor equilibrium point becomes nonideal. When the isentrope enters the two-phase liquid–vapor domain, condensation of the gas phase sets in. At higher levels of energy deposition, the isentropic expansion may be attended by even more exotic effects with a strong variation of the plasma ionization degree  $\alpha$  and nonideality parameter  $\Gamma$ . In one experiment, the thermodynamic para-

eters of matter can vary over a broad range, up to six orders of magnitude in pressure and up to four orders of magnitude in density.

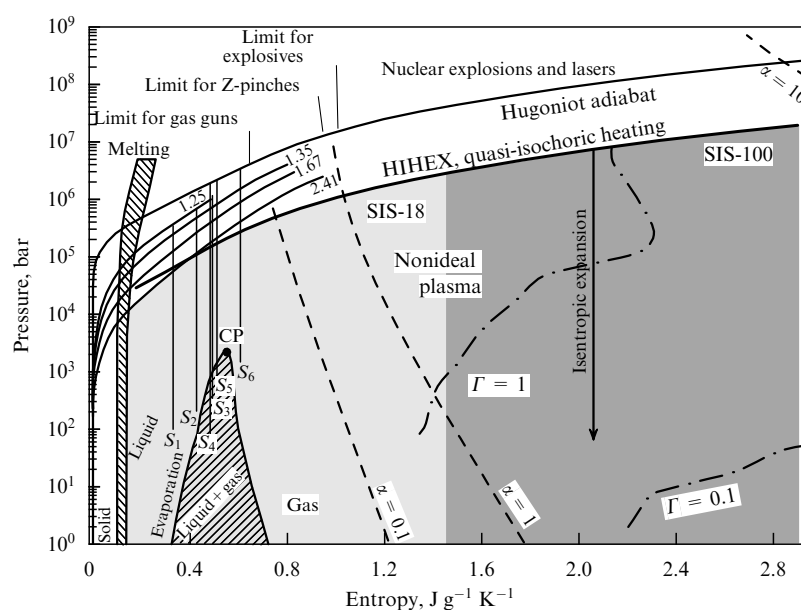
In the pressure–entropy diagram in Fig. 13, the states of matter with a high energy density [56], including the hot compressed ionized substance, the nonideal plasma, the hot expanding liquid, and the quasi-ideal plasma, occupy a vast domain.

Presently available information about the metal properties obtained by the method of isentropic expansion of shock-compressed material [57] is concentrated primarily along the Hugoniot curve and is supplemented with model estimates of the location of critical points in the phase plane (see Fig. 13). That is why the vast domain of the phase diagram under the Hugoniot curve, including domains with the critical points of metals and the nonideal plasma domain ( $\Gamma \geq 1$ ), require further investigations [58–61].

The phase diagram domains corresponding to parameters attainable with the SIS-18 and SIS-100 heavy-ion accelerator facilities are shown in grey and dark grey. In particular, the SIS-18 operating accelerator produces a heating uranium ion pulse with an intensity of  $\approx 10^{10}$  particles, duration of  $\approx 100$  ns, and an ion energy of 300 MeV/nucleon. When this pulse is focused onto a target, the specific energy deposition is at a level of  $\approx 1$  kJ g<sup>-1</sup>. Planned for the future is an increase in beam intensity to raise the specific energy deposition to the level of 10 kJ g<sup>-1</sup>. The TWAC–ITEP accumulator–accelerator put in service at ITEP in 2003 is aimed at reaching the energy deposition level  $\approx 10$ –20 kJ g<sup>-1</sup> by concentrating on a target pulses of copper or cobalt ions with energies up to 700 MeV/nucleon. The new SIS-100 accelerator at FAIR will provide the specific energy deposition level above 100 kJ g<sup>-1</sup>.

Therefore, the development of heavy-ion accelerator drivers will furnish new possibilities for investigating the difficult-to-attain domains of the phase diagram of different substances, which vary greatly in their physical properties.

Figure 14 shows the HIHEX experiment schematic, in which a cylindrical target is bulk-heated by a high-intensity heavy-ion beam. The heated substance (plasma) starts isentropically expanding into the surrounding vacuum. The

**Figure 13.** Pressure–entropy diagram of matter states [56]. (CP is the critical point.)

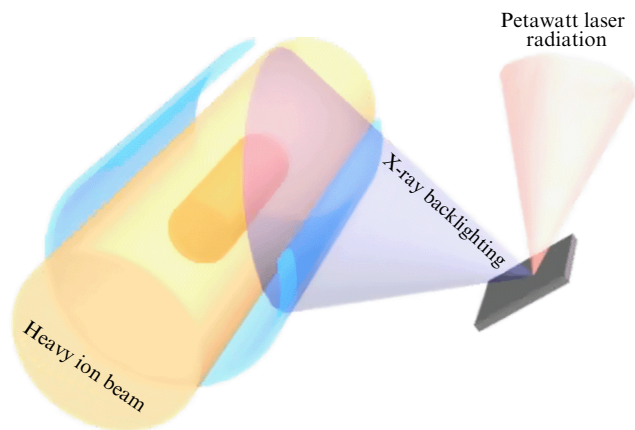


Figure 14. Schematic of the HIXEX experiment.

expansion parameters required for constructing the equations of state of materials are measured using diagnostic systems that involve X-ray backlighting produced by a petawatt laser.

## 6.2 LAPLAS experiment

The LAPLAS experiment implements the strong matter compression mode by cylindrical implosion onto a cylinder axis. The interest in this effect is generated by the feasibility of a laboratory generation of the planetary states of matter existing in the central parts of Jupiter and Saturn, where the substance has a density of  $1\text{--}2\text{ g cm}^{-3}$  at a pressure of  $5\text{--}10\text{ Mbar}$  and a temperature of several electronvolts. Furthermore, the experiment touches on the problem of inertial confinement nuclear fusion driven by a heavy-ion accelerator [1, 62]. As a rule, the targets are cylindrical layered structures with layers of various densities (Fig. 15).

The central area is occupied by a substance (for instance, hydrogen or the equimolar mixture of deuterium and tritium) that should be compressed to as high a density as possible. The substance layer (the absorber) that absorbs the energy of ions is irradiated by a specially shaped hollow beam, which is an annulus in cross section. A solution of the hollow ion beam generation problem was proposed in Refs [62, 64] by RF-field beam rotation at the stage of accelerator-to-target transport. Several design-theoretical studies are dedicated to the search for optimal conditions to provide the uniformity of a hydrodynamic absorber response to the energy deposition induced by this rapidly rotating beam [64, 63]. In this case, special emphasis is placed on the selection of the parameters of the heating ion beam pulse and the geometric dimensions of target layers and their initial densities to provide a nearly adiabatic mode of fuel compression on the cylinder axis [66–69] (see also Refs [70, 71])—the so-called quasi-isentropic mode.

The objective of the LAPLAS experiment [63, 64] is to study the metallization of hydrogen, which is typical for the inner layers of Jupiter and Saturn. A two-dimensional hydrodynamic code [72] was used to perform numerical feasibility investigations of the quasi-isentropic compression mode under the action of a heavy-ion beam to realize the effect of hydrogen metallization, which was predicted by Wigner and Hugoniot back in 1935. The numerical simulations dealt with a multilayer cylindrical target with a length and external radius of  $3\text{ mm}$  each (see Fig. 15). The radius of the internal cylinder, which consisted of solid frozen hydrogen, was equal to  $0.5\text{ mm}$ . The cylinder face is

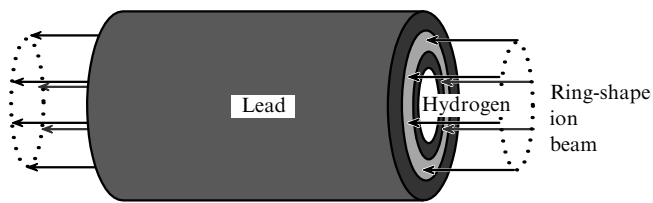


Figure 15. Structure of a multilayer cylindrical target for the LAPLAS experiment [63].

irradiated by a beam of  $10^{12}$  uranium ions with an energy of  $400\text{ MeV/nucleon}$  and a pulse duration of  $50\text{ ns}$ . An important point is the annular structure of the beam section: the beam is focused into a ring with inner and outer radii of  $2.0$  and  $0.5\text{ mm}$ , and irradiates a cylindrical layer of lead rather than hydrogen. The energy deposition is assumed to be uniform lengthwise through the lead layer, because the range of  $400\text{ MeV/nucleon}$  uranium ions in lead amounts to  $4.25\text{ mm}$ , with the consequence that the Bragg peak is beyond the target.

A characteristic feature of the experiment consists in the mode of generation of a series of reverberating weak shock waves, which compress hydrogen along the isentrope. The BIG two-dimensional hydrodynamic code [72] enables calculating the hydrogen density distribution along the cylinder radius at different time instants. According to the simulation data, for a relatively slow adiabatic motion of the hydrogen–lead interface toward the cylinder axis, a series of weak reflected shock waves emerges between this interface and the axis. Under the action of these shocks, the substance transforms into a state that corresponds to the metallization of hydrogen. In accordance with the equation of state from the SESAME table, this is the pressure  $3\text{ Mbar}$ , the density  $\sim 1\text{ g cm}^{-3}$ , and the temperature  $\geq 0.1\text{ eV}$  [63]. These parameters remain invariable for  $160\text{--}200\text{ ns}$ , which is quite sufficient for measuring the conductivity of hydrogen under extreme conditions. Recent experiments in the quasi-adiabatic compression of hydrogen [1, 2] suggest that the pressure-induced metallization occurs at pressures about  $1\text{ Mbar}$  and densities  $\approx 0.6\text{ g cm}^{-3}$ .

## 6.3 WDM experiment

The WDM experiment is targeted at realizing the quasi-isochoric mode of matter heating and attaining the extreme plasma state involving a strong interparticle interaction for large values of the nonideality parameter,  $\Gamma \geq 1$  [2].

The physical substantiation of the experiment to be performed with the ion beams of the SIS-100 accelerator, which is under development in the framework of the FAIR project, is outlined in Ref. [73]. The experiment is aimed at the study of the solid hydrogen state for the energy deposition level of  $130\text{ kJ g}^{-1}$ , which is afforded by a  $200\text{ MeV/nucleon}$  uranium ion beam with an intensity of  $8 \times 10^{10}$  focused on a spot of the radius  $r_b = 350\text{ }\mu\text{m}$  (the rms value). According to the equation of state from the SESAME tables, this corresponds to the temperature  $0.6\text{ eV}$ —the mode of ‘warm dense matter’, in which the entire beam energy is converted to the internal energy of matter.

In the case of volumetric energy deposition by an ion beam, characteristic of ions with energies  $E \geq 10\text{ MeV/nucleon}$ , the energy deposition  $E_s$  is the governing characteristic, which can be measured with good accuracy. And if the

sample density  $\rho_0$  remains invariable during heating, the thermodynamic parameters of matter after irradiation are defined by  $\rho_0$  and  $E_s$ . Therefore, any measurable physical quantities are functions of the characteristics of this well-defined thermodynamic state.

The choice of the target material is determined by the capabilities of the diagnostic technique, which involves recording the spectral and angular distribution of X-ray photons scattered by the substance of the heated sample—the Thomson X-ray scattering method [74]. This X-ray backlighting with temporal resolution can be provided by the PHELIX (Petawatt High-Energy Laser for Heavy Ion Experiments) laser, which is under construction at the GSI [1, 75]. For X-ray photon energies  $\approx 1\text{--}3\text{ keV}$ , the choice of target structure materials is nevertheless limited to elements with a low atomic number  $Z$ . To carry out the diagnostics of the state of matter and interpret the data, it is advisable to deal with a uniform density distribution in the bulk of the sample. The simplest target for the execution of a quasi-isochoric experiment is a cylinder of frozen hydrogen of radius  $R_H \geq r_b$  (Fig. 16). For a rectangular intensity distribution over the beam section, the density on the cylinder axis remains constant until the unloading wave reaches the axis. However, for a realistic beam with a Gaussian intensity distribution over its section, for which the second derivative of the pressure with respect to radius is nonzero, the density begins to decrease even prior to the arrival of the unloading wave at the axis.

Such an effect of hydrodynamic unloading of the heated target domain may be compensated by an inert shell (tamper) limiting the frozen hydrogen. To provide the requisite ‘confinement’ of the heated matter by a low- $Z$  material transparent to X-ray photons, the tamper is also heated by the peripheral part of the ion beam. In this case, the heated layer of the tamper produces counterpressure for confining the main substance of the target. Clearly, it is advantageous to use a material with a high sublimation energy as a tamper to delay the onset of the hydrodynamic expansion of the tamper itself.

Numerical simulations performed using the BIG-2 two-dimensional hydrodynamic code [72] suggest that the tamper density should be lower than that of graphite. That is why a plastic with a density of  $1.5\text{ g cm}^{-3}$  at normal conditions was selected as the tamper material. The temporal variation of the target layer densities is shown in Fig. 17. Owing to the

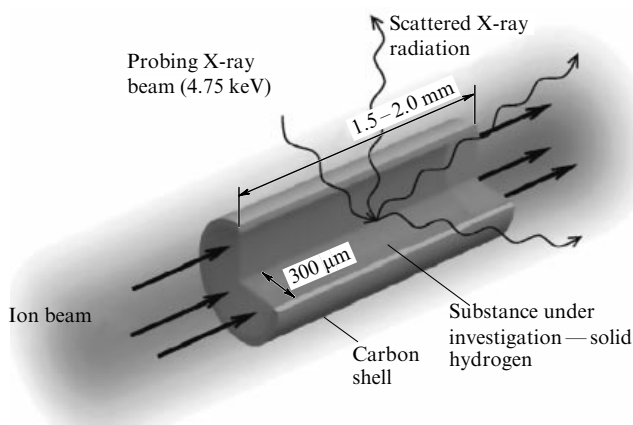
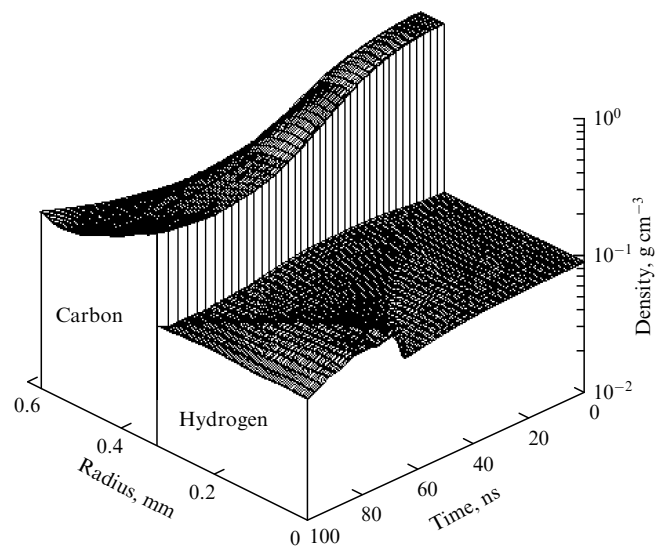


**Figure 16.** WDM. Schematic of an experiment on the isochoric heating of hydrogen [73].

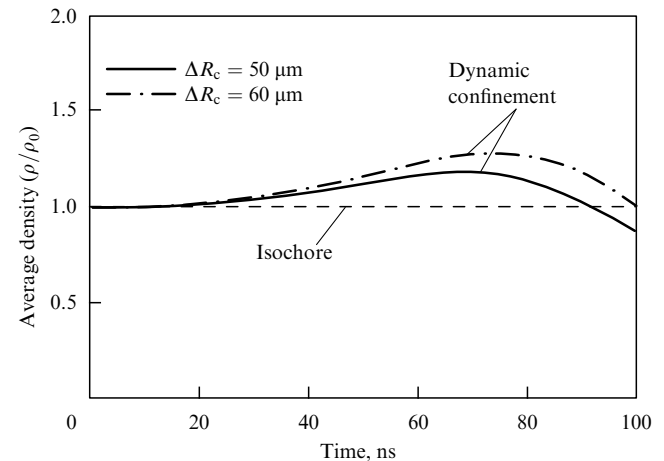
Gaussian profile of the ion beam, the hydrogen density initially begins to decrease. The pressure in the tamper material exceeds that of hydrogen, and therefore the tamper begins to move inward and produces a weak shock wave. Later on, when the tamper density decreases, the pressure equalizes and the hydrogen–tamper interface stops. Then the increasing hydrogen pressure returns the interface to its initial position. According to simulations, by the end of the ion irradiation, the radial density distribution is nearly uniform.

Figure 18 shows the time evolution of the hydrogen density averaged over the target cross section. The tamper thickness  $\Delta R_c$  can be optimized depending on the result required: minimization of density variations during heating to within 10%–15% ( $\Delta R_c = 50\text{ }\mu\text{m}$ ) or attainment, by the end of irradiation, of the hydrogen density equal to the initial density  $0.1\text{ g cm}^{-3}$  ( $\Delta R_c = 60\text{ }\mu\text{m}$ ).

Thus, it has been shown that for a prescribed set of initial parameters, an ion beam is capable of ensuring a quasi-isochoric heating mode of solid-density hydrogen for a temperature of  $5000^\circ\text{C}$ , i.e., of providing dynamic confinement for 100 ns.



**Figure 17.** Time dependence of the densities of target layers [30].



**Figure 18.** Time evolution of hydrogen density averaged over the target cross section [73].

## 7. Atomic physics with relativistic beams of highly charged ions and antiprotons

Virtually all of the main capabilities of FAIR will be realized in experiments—high-intensity beams of stable ions in different charge states in the velocity range from zero to nearly the speed of light ( $v \sim 0.99c$ ), as well as ultracold antiprotons. Furthermore, not only ordinary targets but also extraordinary ones like ultracold electrons, atoms, molecules, or clusters will be used, which can be irradiated by high-intensity light fields produced by high-power lasers.

Atomic physics research on the FAIR accelerator complex focuses on three main issues.

1. The physics of extremely strong electromagnetic fields emerging with the use of stored ion beams is the main subject of the Stored Particle Atomic physics Research Collaboration (SPARC) [76]. It is planned to carry out high-precision experiments with the heaviest relativistic ions to study their electron structure and the internal dynamics of electron shells in detail. The data of these experiments will allow a substantive conclusion about the applicability of the basic theory of matter–light interaction in extremely strong fields. In experiments of the first type, the heaviest relativistic ions will be used for investigating the interaction of highly ionized atoms with electrons and photons under the conditions of a rapidly time-varying superstrong electromagnetic field for large values of the relativistic Doppler shift [76, 77]. In this case, it becomes possible to overcome the critical field intensity for the spontaneous production of lepton pairs ( $e^+e^-$ ) (of the order of  $10^{16} \text{ V cm}^{-1}$ ), the so-called Schwinger limit [78]. For illustration, Fig. 19 shows the angular intensity distribution of the radial electric field produced by a point-like charge traveling at relativistic velocities [76].

As is clear from Fig. 19, as the charge velocity approaches the speed of light, the electric field in the direction transverse to the direction of motion increases, while the longitudinal field component decreases  $\sim \gamma^{-2}$ . In this case, the time of interaction with a target atom with an impact parameter  $b \sim 10^6 \text{ fm}$  is about 0.1 as ( $10^{-19} \text{ s}$ ). Therefore, it becomes possible to measure the dependence of the impact parameter of the interaction on both the longitudinal and transverse field components for the ionization of atomic inner shells and their excitation. These experiments will require the use of high-precision spectroscopic techniques for recording photon, electron, and positron emissions, which yield the desired information about the excitation mechanisms in the superstrong fields at issue.

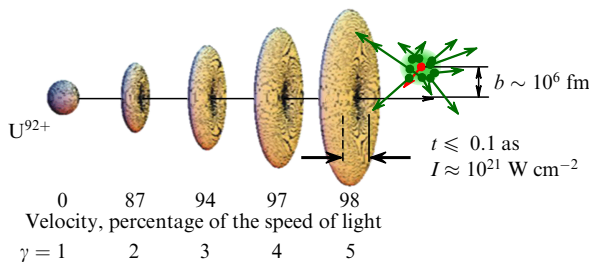


**Figure 19.** Angular intensity distribution of the radial electric field produced by a point-like charge traveling at relativistic velocities (Lorentz factor  $\gamma$  ranging from 1 to 5 in the laboratory frame of reference) [76].

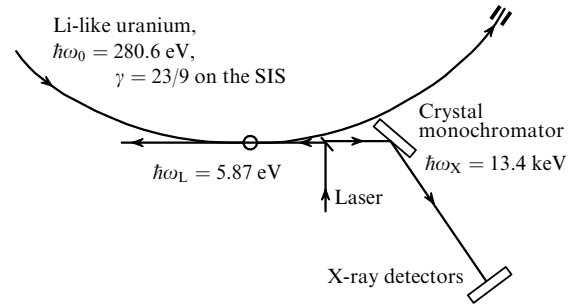


**Figure 20.** Schematic of an experiment for measuring the hyperfine structure of Li-like heavy ions [76].

It is noteworthy that Lorentz factors  $\gamma$  ranging from 1 to  $\sim 30$  can be realized with different FAIR storage rings. Therefore, the electric field intensity in the interaction with target atoms can exceed the intensity of the field retaining 1s electrons in the K shell of uranium atoms ( $\sim 10^{16} \text{ V cm}^{-1}$ ) [76].

2. Another type of the SPARC experiment is aimed at attaining high-ion-charge states, up to the production of fully stripped uranium nuclei circulating in the SIS-100 synchrotron ring. The objective is a high-precision verification of quantum electrodynamics in extremely high electric fields. In this case, it is required to measure corrections to the fine structure of one-, two-, and three-electron atoms, especially for the  $1s_{1/2}$  and  $2s_{1/2}$  states. For Li-like heavy ions, it becomes possible to directly excite the  $2s$ – $2p$  transitions through the use of the Doppler effect, where a laser beam is directed in opposition to the relativistic ion beam (Fig. 20) [76].

As a result of laser excitation, the emitted photon will be Doppler-shifted (in proportion to  $2\gamma$ ), which will permit performing high-sensitivity measurements with a reliable suppression of scattered primary photons. In particular, the 230 eV transition energy in uranium for  $\gamma = 23$  can be measured with the record high precision  $\pm 0.007 \text{ eV}$ . The interaction of laser radiation and the heavy-ion beam circulating in the ring will be used for efficient-beam cooling, up to the emergence of an ordered ion structure in the beam—the production of so-called crystal beams of highly charged heavy ions [79].

These experiments will be carried out on the new NESR with the use of the PHELIX petawatt laser and the SIS-300 synchrotron ring [75].

Unlike experimental facilities typical for this area of physics, the storage ring permits accurate control over the charge state composition of the beam and the diagnostics of the final states of atoms and electrons at a level of single particles and events. This signifies the feasibility of forming unique unperturbed controllable conditions whereby one ion, the laser radiation field, and one electron participate in the interaction. Therefore, investigations will be made of the fundamental quantum electrodynamic corrections to binding energies in atoms, the magnetic moment, and magnetic interaction in the ultrahigh-field regime. The investigations will be carried out using an X-ray crystal spectrometer, a low-temperature calorimeter, a Compton polarimeter, an electron spectrometer, and other diagnostic systems with a large acceptance, which will allow verifying quantum-electrodynamic models from spectroscopic data on sequential atomic transitions [77, 80].

## 8. Atomic physics at a facility for low-energy antiproton and ion research (FLAIR)

The subjects of experimental research planned by the FLAIR (Facility for Low-energy Antiproton and Ion Research) collaboration include studies of fundamental symmetries, the effect of gravity on antimatter, matter–antimatter interactions, and the physics of antimatter atoms.

The FLAIR facility complex [81] comprises new-generation facilities for the generation of ultracold antiproton beams that are required for the highest-resolution spectroscopic investigations of laser-cooled trapped atoms of antihydrogen and antihelium [81]. The antiproton beams generated with the effective intensity up to  $\approx 10^{12} \text{ s}^{-1}$  will enable decelerating and trapping antiprotons in amounts 100 times greater than those presently obtained at CERN [82].

The antiprotons produced in the interaction of a high-intensity 29 GeV proton beam with a thick ( $\approx 8 \text{ cm}$ ) generating iridium target [83] are directed to the CR (see Section 2), where they experience cooling at an energy of 3 GeV. Subsequently, the intensity of antiprotons increases in the RESR, from which they are directed to the NESR to be decelerated to an energy of 30 MeV. Further antiproton deceleration to energies required for experiments (from 0 to 5 MeV) is effected by decelerating the initially fast antiproton beam in two sequential storage rings: in the LSR (Low-energy Storage Ring) magnetic ring (30 MeV–300 keV) and the USR (Ultra-low energy Storage Ring) electrostatic ring (300 keV–20 keV) [6] (Fig. 21).

In the LSR and USR, which use electron cooling to provide low emittance values ( $\epsilon \approx \pi \text{ mm mrad}$ ,  $\Delta p/p \approx 10^{-4}$ ), internal gaseous targets for investigating atomic collisions with antiprotons are installed. A Penning trap in the HITRAP universal facility [84] is used to cool and decelerate antiprotons down to their full stop.

The availability of such a low-energy antiproton beam opens up new experimental possibilities that have not been realized anywhere in the world. For instance, an ultrahigh-precision spectroscopy of the 1.4-GHz line arising from the hyperfine splitting of the ground state of antihydrogen with a relative accuracy of  $10^{-4}$  ( $\Delta \nu \approx 100 \text{ kHz}$ ) or of the 2.5 GHz hyperfine splitting of the 1s–2s transition with a relative accuracy of about  $10^{-10}$  will permit reaching the sensitivity

required for detecting the CPT invariance violation [85–87] and verifying the data of QED calculations [88].

Laser-cooled trapped antiprotons open up the way to the experimental investigation of the effect of gravity on antimatter; earlier investigations were hampered by the fact that gravitational effects were covered by the electromagnetic interaction, which was many orders of magnitude stronger. Projected for this purpose is the execution of corresponding high-sensitivity experiments on cooled neutral antihydrogen atoms [89].

Collision experiments with antiprotons and antihelium will permit making a complete reconstruction of collisional processes for the first time. Owing to the availability of a continuously extracted beam, it will be possible to measure the X-ray spectra of antiprotonic atoms and study nucleus–antinucleus scattering, for instance, with large antimatter systems like a positively charged antihydrogen atom  $\bar{\text{H}}^+$  (one antiproton and two positrons). Furthermore, combining unstable nuclei and antiprotons as probe particles in a single facility opens up fresh possibilities for studying the structure of exotic nuclei.

## 9. Radiative study of materials and biophysics (BIOMAT)

Heavy-ion beams at the FAIR accelerator complex with the energy above 10 GeV/nucleon are of immediate interest for the study of radiation influence of galactic and solar particles on living biological subjects, as well as on various materials. The area of practical applications includes the radiative study of materials, in particular radiation resistance tests of microelectronic components, nuclear medicine (simulation of the cosmic radiation effect of heavy charged particles on living cells), etc. In this case, of special significance in the formulation and execution of these experiments is the property of fast ions to penetrate to a controllable depth inside the samples.

### 9.1 Biophysical experiments

Comprehensive data about the radiological effects of fast heavy charged particles on living organisms are required for decreasing the thickness of expensive radiobiological shielding on interplanetary mission spacecraft to the minimal necessary level [90, 91]. Furthermore, a facility developed for sample irradiation is required for testing and calibrating different instruments and equipment employed in space.

Cosmic radiation of solar and galactic origin poses the greatest hazard in interplanetary space investigations and in manned interplanetary missions because the personnel and instrumentation are outside of the protective terrestrial magnetic field [91, 92]. Genetic changes and oncological effects may emerge even for low irradiation levels. However, in the case of a solar flare and coronal mass ejection, the lethal dose may be accumulated in less than 30 min. While solar radiation consists primarily of protons and helium nuclei, galactic radiation also comprises heavier particles up to iron. Thus, because the radiation influence is determined by stopping energy loss, which is proportional to the squared particle charge in accordance with the Bethe–Bloch formula [1, 93], the risk coefficient for the emergence of an oncological disease (Fig. 22) [90] under irradiation by relativistic iron ions is three orders of magnitude higher than under proton irradiation.

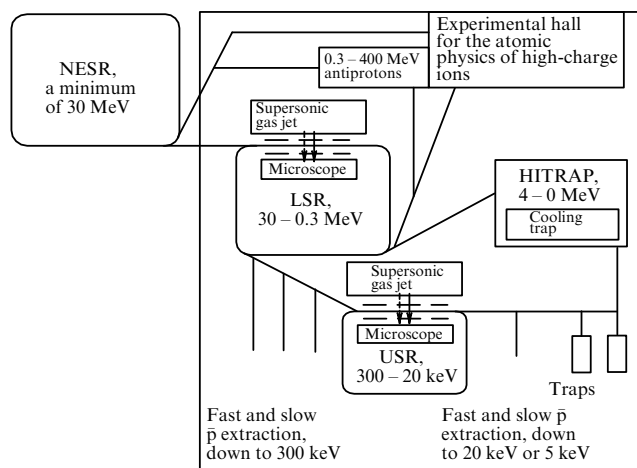


**Figure 21.** Arrangement of experimental facilities in the FLAIR building [80].



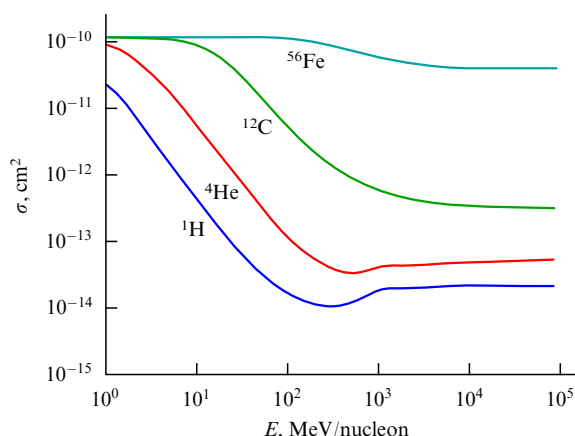


**Figure 22.** Calculated risk coefficient for the emergence of malignant neoplasms in mammary gland cells under the long-term action of heavy charged particles [90].

The dose is the main factor for both living organisms and electronic devices. Usually, the dose is macroscopically defined as the energy absorbed by a unit mass [ $1 \text{ J kg}^{-1} = 1 \text{ Gray (Gy)}$ ]. However, of higher significance is the local dose distribution along an individual particle track [94], which amounts to many kilograms at the track center. It is precisely this disproportionately strong response to relatively low macroscopic doses that is observed in many biological systems. This effect of higher radiobiological efficiency (RBE) [95, 96] is attributed to numerous kinds of damage caused to both strands of deoxyribonucleic acid (DNA) in the vicinity of a heavy charged particle track. The RBE and the effect of fragmentation of a heavy relativistic particle in its stopping are responsible for enhanced transformation of cells irradiated by iron ions, despite a low intensity in comparison with the proton beam intensity.

In the experiments due to be executed at FAIR, special emphasis will be placed on the effect of relativistic nuclei fragmentation and the resultant shower of secondary low-energy particles with a high RBE for living subjects. Since the secondary particles are correlated in space and time, it is planned to investigate the radiobiological effect not only at the genetic molecular level but also at the cell level of living tissues [97].

## 9.2 Experiments in material science

Experiments on the FAIR accelerator in the simulation of the influence of the heavy component of galactic cosmic radiation on materials pursue two primary goals:

(i) calibration of spacecraft instrumentation used to detect high-energy ( $> 1 \text{ GeV/nucleon}$ ) cosmic particles with a high resolution in particle mass and charge;

(ii) study of radiation effects in electronic components used in the instrumentation of space satellites — from single chips to microprocessors [98]. Such effects are responsible for single failures, the occurrence of destructive operational errors, or the disabling of critical functions of spaceborne electronics.

Heavy ions obtained from the SIS-100 will be used in the multipurpose BIOMAT facility equipped with a raster scanning system [99], which will provide an excellent beam quality in the uniform irradiation of a large-surface field in a broad intensity range for particles of different atomic masses. A special robot will be used for positioning the samples [4].

A broad set of ion beams — from proton to uranium ones — will be required for biophysical and material research. The highest requisite beam intensities for an energy of  $10 \text{ GeV/nucleon}$  in the ion mass range from protons ( $5 \times 10^{10} \text{ cm}^{-2}$ ) to iron ( $1 \times 10^8 \text{ cm}^{-2}$ ) correspond to a dose of  $10 \text{ Gy}$  uniformly absorbed in  $1 \text{ min}$  by a target  $100 \text{ cm}^2$  in area. Acceptable irradiation times can be achieved for this dose rate, which is highly significant in the irradiation of sensitive biological samples (i.e., cell cultures), which should be in a nutrient medium. The highest intensities of heavier-ion beams — from krypton to uranium ones ( $1 \times 10^8 \text{ cm}^{-2}$ ) — are determined by the fluxes required for material research in combination with reasonable exposure times.

The BIOMAT collaboration will use the high-energy ion guide and the experiment site jointly with the SPARC collaboration. Fourteen research groups participate in the collaboration.

## 9.3 Experiments on the modification of materials by relativistic heavy ion beams

In passing through a solid material, high-energy heavy ions induce ultrahigh electric fields (of the order of  $10^{12} \text{ V m}^{-1}$ ) in short time intervals ( $\sim 10^{-18} \text{ s}$ ), which affect atoms and electrons in the vicinity of their path of motion, converting the kinetic energy of fast particles into the internal energy of matter. The energy loss excites complicated processes like the generation of fast electrons, which is attended by the Coulomb repulsion of ionized atoms, the emission of X-ray photons and Auger electrons, electron–phonon interaction, etc. [100–102]. As a result, a fast particle can produce long cylindrical zones several nanometers in radius, in which the properties of matter are significantly different from the initial ones. For example, we can note the crystalline-to-amorphous state transition or the formation of metastable high-pressure high-temperature phases [101, 102].

Studying the transient processes initiated by the passage of a fast particle through matter is most important for explaining the track formation mechanisms (Fig. 23) [103].

In particular, electron processes prevail in the track evolution in the time interval from  $\sim 10^{-18} \text{ s}$  to  $\sim 10^{-13} \text{ s}$ . Diagnosing the damage process with a high resolution (at a the level of  $10^{-14} \text{ s}$ ) can be achieved by detecting convoy electrons and Auger electrons or by X-ray techniques [2, 3]. However, the complete picture of track formation mechanisms involving displacements of atoms due to the excitation by electrons includes slower processes ( $\sim 10^{-13} - 10^{-12} \text{ s}$ )

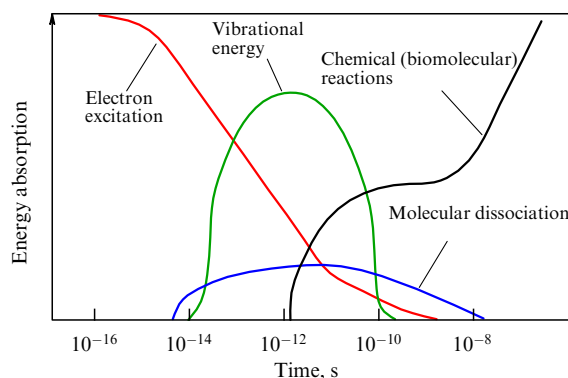


**Figure 23.** Temporal diagram of energy dissipation in a polymer sample after the passage of a charged particle [103].

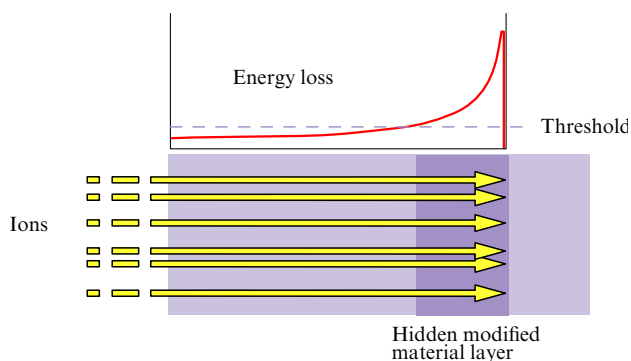


**Figure 24.** Material modification in the region of the Bragg peak in a precompressed sample [103].

related to the passage of a shock wave and lattice relaxation [104, 105].

The most important quantitative characteristic used in the description of fast-particle stopping in a solid substance is the stopping power  $dE/dx$  (the energy loss per unit path length). For nonrelativistic ions ( $E_i < 1$  GeV/nucleon), the stopping mechanisms have been comprehensively studied theoretically and experimentally [106, 107]. However, for relativistic ions with energies  $E_i > 2$  GeV/nucleon, the experimental data on the stopping power are quite scarce.

Among the experimental problems in material science to be solved at the FAIR facility is the study of modifications of solids precompressed to a pressure of 25 GPa, in the bulk of which a high-intensity heavy-ion beam is decelerated. The idea of the experiment is to study phase transformations of a substance, which is compressed using diamond anvils, in the vicinity of the Bragg peak, where the stopping power is highest [106, 107] (Fig. 24).

Heavy ions release energy in a small volume during a short period of time to provide the threshold structural change of a solid substance, which was in a subthreshold state due to precompression. Furthermore, the ion beam generates acoustic waves in the sample, which also affect the phase transition processes. Therefore, the combination of high pressure and the local energy deposition by a fast-ion beam will create the opportunity to generate those phase transitions that cannot occur under the application of pressure alone. In these investigations, it is planned to use several promising diagnostic techniques, including X-ray and neutron diffraction, Raman spectroscopy, and the resonance measurements of muon spin [108].

## 10. Conclusions

The FAIR project is of significant scientific and practical interest to the Russian scientific community and opens the possibility for acquiring new fundamental knowledge about the structure and properties of matter, educating young scientists and engineers, and developing information technologies. The experiments to be made at FAIR will enable a new step in the study of nuclear structure owing to the use of beams of stable ions and of short-lived (radioactive) nuclei away from the stability range.

The combination of the high intensity and high phase density of heavy-ion beams will allow investigating the deconfinement of quarks and the properties of the quark–gluon plasma in new, previously unattainable domains of the phase diagram of nuclear matter.

The use of high-intensity antiproton beams will lend new impetus to investigations of hadron structure and strong interactions in the framework of QCD.

The unique combination of high-intensity pulsed heavy-ion beams and the radiation of a petawatt laser will permit executing experiments in the physics of superdense nonideal electromagnetic plasma in the phase-diagram domains of extreme matter states that are hardly attainable via other experimental techniques.

Atomic physics, quantum electrodynamics in superhigh electromagnetic fields, and applied research in the radiative study of materials, medicine, and biology will advance further with the FAIR facilities with the use of highly charged heavy ion beams and antiproton beams.

Even with the start version of the project [109], investigations will be carried out on a unique research complex.

In the course of Russia's participation in the FAIR project, the main investments will be made in the development of the institutes involved in the project, as well as in the enterprises that deliver high-technology products. During the construction of the accelerator complex, Russian research institutions and industrial enterprises will receive contracts for the development and fabrication of high-technology components of experimental detectors and accelerator components and will gain access to foreign high technologies.

**Acknowledgments.** The authors express their appreciation to A N Skriskii, R Bock, P Senger, I N Meshkov, H Gutbrod, and O O Patarakin for the helpful discussions, as well as to V L Varentsov for his highly competent expertise, instructive discussions, and support in the selection and preparation of the material for publication.

## References

1. Fortov V E, Hoffmann D H H, Sharkov B Yu *Usp. Fiz. Nauk* **178** 113 (2008) [*Phys. Usp.* **51** 109 (2008)]
2. Fortov V E *Ekstremal'nye Sostoyaniya Veshchestva na Zemle i v Kosmose* (Extreme States of Matter on Earth and in the Cosmos) (Moscow: Fizmatlit, 2008) [Translated into English (Berlin: Springer, 2011)]
3. ESFRI, the European Strategy Forum on Research Infrastructures, [http://ec.europa.eu/research/infrastructures/index\\_en.cfm?pg=esfri](http://ec.europa.eu/research/infrastructures/index_en.cfm?pg=esfri)
4. Gutbrod H H (Ed.-in-Chief), FAIR Baseline Technical Report (Darmstadt: GSI, 2006)
5. Parkhomchuk V V, Skriskii A N *Usp. Fiz. Nauk* **170** 473 (2000) [*Phys. Usp.* **43** 433 (2000)]
6. Van der Meer S, Preprint CERN/ISR PO 72-31 (Geneva: CERN, 1972)
7. Mohl D, CAS-87, CERN 87-03 (1987)
8. Golovkov M S et al. *Phys. Lett. B* **672** 22 (2009)
9. Neidherr D et al. *Phys. Rev. Lett.* **102** 112501 (2009)
10. Sun B et al. *Int. J. Mod. Phys. E* **18** 346 (2009)
11. Nörtershäuser W et al. *Phys. Rev. Lett.* **102** 062503 (2009)
12. Nakamura T et al. *Phys. Rev. A* **74** 052503 (2006)
13. Rubio B, Nilsson T *Nucl. Phys. News* **16** (1) 9 (2006)
14. Tanihata I et al. *Phys. Rev. Lett.* **55** 2676 (1985)
15. Orr N A et al. *Phys. Rev. C* **51** 3116 (1995)
16. Yamazaki T et al. *Z. Phys. A* **355** 219 (1996)
17. Rudolph D et al. *Phys. Rev. C* **78** 021301(R) (2008)
18. Regan P H et al. *Nucl. Phys. A* **787** 491 (2007)
19. Tomaselli M et al. *Hyperfine Interact.* **171** 243 (2006)
20. Nakamura T et al. *Phys. Rev. A* **74** 052503 (2006)
21. Gutbrod H H et al. (Eds) "An international accelerator facility for beams of ions and antiprotons", Conceptual Design Report (Darmstadt: GSI, 2001) p. 12; <http://www.fair-center.eu/fair-users/publications/fair-publications.html>
22. Pfeiffer B et al. *Nucl. Phys. A* **693** 282 (2001)

23. Kratz K-L et al. *Hyperfine Interact.* **129** 185 (2000)
24. Winkler M et al. *Eur. Phys. J.* **150** 263 (2007)
25. Scheidenberger C et al. *Nucl. Instrum. Meth. Phys. Res. B* **204** 119 (2003)
26. Herfurth F et al. *Int. J. Mod. Phys. E* **18** 392 (2009)
27. Schwarz S et al. *Nucl. Instrum. Meth. Phys. Res. B* **204** 507 (2003)
28. Neumayr J B et al. *Nucl. Instrum. Meth. Phys. Res. B* **244** 489 (2006)
29. Radon T et al. *Phys. Rev. Lett.* **78** 4701 (1997)
30. Litvinov Yu A et al. *Nucl. Phys. A* **756** 3 (2005)
31. York R C *Physica C* **441** 31 (2006)
32. Kester O et al. *Nucl. Instrum. Meth. Phys. Res. B* **204** 20 (2003)
33. Mittag W, Villari A C C *Eur. Phys. J. A* **25** (Suppl. 1) 737 (2003); in *4th Intern. Conf. on Exotic Nuclei and Atomic Masses, ENAM'04, Pine Mountain, Georgia, September 2004*
34. Loiselet M et al., in *Cyclotrons and their Applications: 14th Intern. Conf., Cape Town, South Africa, 8–13 October 1995* (Ed. J C Cornell) (Singapore: World Scientific, 1996) p. 629
35. Habs D et al. *Nucl. Instrum. Meth. Phys. Res. B* **204** 739 (2003)
36. Hofmann S, Münzenberg G *Rev. Mod. Phys.* **72** 733 (2000)
37. Goto A, Yano Y, Katayama T *J. Phys. G Nucl. Part. Phys.* **24** 1341 (1998)
38. Report of the NSAC Subcommittee on Comparison of the Rare Isotope Accelerator (RIA) and the Gesellschaft für Schwerionenforschung (GSI) Future Facility, 2004, [http://science.energy.gov/~media/np/nsac/pdf/docs/ria\\_gsi\\_nsac\\_022604.pdf](http://science.energy.gov/~media/np/nsac/pdf/docs/ria_gsi_nsac_022604.pdf)
39. FAIR — Baseline Technical Report, Vol. 3A. Experiment Proposals on QCD Physics. 3.1 CBM (2006) p. 1; [http://www.fair-center.eu/fileadmin/fair/publications\\_FAIR/FAIR\\_BTR\\_3a.pdf](http://www.fair-center.eu/fileadmin/fair/publications_FAIR/FAIR_BTR_3a.pdf)
40. Senger P “Status of the CBM experiment at FAIR”, in CBM Progress Report 2009 (Eds F J Müller, V Fries) (Darmstadt: GSI, 2010) p. 1; <http://www.gsi.de/documents/DOC-2010-Apr-17-1.pdf>
41. Dremin I M *Usp. Fiz. Nauk* **179** 571 (2009) [*Phys. Usp.* **52** 541 (2009)]
42. Friman B L, Hohne C, Rapp R (Eds) *Strongly Interacting Matter: The CBM Physics Book* (Lecture Notes in Physics, Vol. 814) (New York: Springer, 2010)
43. Detector CBM, <http://www.gsi.de/fair/experiments/CBM/detector.html>
44. Atoyan G S et al. *Nucl. Instrum. Meth. Phys. Res. A* **320** 144 (1992)
45. Bumazhnov V et al. *Prib. Tekh. Eksp.* (4) 77 (1999) [*Instrum. Exp. Tech.* **42** 505 (1999)]
46. Föhl F *Eur. Phys. J.* **162** 213 (2008)
47. Bartoszek L et al. “Proposal 986: Medium-energy antiproton physics with The Antiproton Annihilation Spectrometer (TAPAS\*) at Fermilab”, [http://www.fnal.gov/directorate/program\\_planning/Nov2010PACPublic/986\\_TAPAS\\_Proposal\\_2010\\_11\\_10.pdf](http://www.fnal.gov/directorate/program_planning/Nov2010PACPublic/986_TAPAS_Proposal_2010_11_10.pdf)
48. Ekström C “Internal targets”, CERN Report 92-01 (Geneva: CERN, 1992) p. 120
49. Reich H et al. *Nucl. Phys. A* **626** 417 (1997)
50. Trostell B *Nucl. Instrum. Meth. Phys. Res. A* **362** 41 (1995)
51. Aleksan R et al. *Nucl. Instrum. Meth. Phys. Res. A* **397** 261 (1997)
52. Novotny R et al. *IEEE Trans. Nucl. Sci.* **47** 1499 (2000)
53. CMS Technical Proposal, CERN/LHCC 94-38, LHCC/P1 (1994)
54. Chiang I H et al. *IEEE Trans. Nucl. Sci.* **42** 394 (1995)
55. PANDA Collab. “Strong interaction studies with antiprotons”, Technical Progress Report for PANDA (2005)
56. Hoffmann D H H et al. *Phys. Plasmas* **9** 3651 (2002)
57. Korobenko V N, Rakhel' A D, Savvatimskii A I, Fortov V E *Fiz. Plazmy* **28** 1093 (2002)
58. Zel'dovich Ya B, Raizer Yu P *Fizika Udarnykh Voln i Vysokotemperaturnykh Gidrodinamicheskikh Yavlenii* (Physics of Shock Waves and High-Temperature Hydrodynamic Phenomena) (Moscow: Nauka, 1966) [Translated into English (Mineola, NY: Dover Publ., 2002)]
59. DaSilva L B et al. *Phys. Rev. Lett.* **81** 224 (1998)
60. Batani D et al. *Europhys. News* **27** 210 (1996)
61. Batani D et al. *Phys. Rev. Lett.* **88** 235502 (2002)
62. Koshkarev D G, Churazov M D *At. Energ.* **91** (1) 47 (2001) [*At. Energy* **91** 564 (2001)]
63. Tahir N A et al. *Phys. Rev. E* **63** 016402 (2001)
64. Piriz A R, Tahir N A, Hoffmann D H H, Temporal M *Phys. Rev. E* **67** 017501 (2003)
65. Basko M M et al. *Laser Part. Beams* **20** 411 (2002)
66. Basko M *Phys. Plasmas* **7** 4579 (2000)
67. Kazarin A et al., GSI-2001-4 Annual Report (2000) p. 48
68. Basko M, Kemp A, Meyer-ter-Vehn J *Nuclear Fusion* **40** 59 (2000)
69. Churazov M D, Sharkov B Yu *Nuovo Cimento A* **106** 1945 (1993)
70. Tahir N A et al. *Contrib. Plasma Phys.* **41** 287 (2001)
71. Tahir N A et al. *Contrib. Plasma Phys.* **43** 373 (2003)
72. Fortov V et al. *Nucl. Sci. Eng.* **123** 169 (1996)
73. Kozyreva A et al., GSI-2003-2 Annual Report (2003) p. 27
74. Gregori G et al. *Phys. Rev. E* **67** 026412 (2003)
75. Kuehl Th et al. *Hyperfine Interact.* **162** 55 (2006)
76. Stöhlker Th et al. *Nucl. Instrum. Meth. Phys. Res. B* **205** 156 (2003)
77. The SPARC Collab. “Technical report for the design, construction, commissioning and operation of the SPARC Project: Stored Particle Atomic Physics Collaboration at the FAIR Facility”, [http://www-linux.gsi.de/~sparc/documents/pdf\\_files/06\\_01\\_06\\_SPARC\\_TR.pdf](http://www-linux.gsi.de/~sparc/documents/pdf_files/06_01_06_SPARC_TR.pdf)
78. Schwinger J *Phys. Rev.* **82** 664 (1951)
79. Maletic D M, Ruggiero A G (Eds) *Crystalline Beams and Related Issues. Proc. of the 31st Workshop, Erice, Sicily, Italy, Nov. 1995* (Singapore: World Scientific, 1996)
80. Schuch R, Stöhlker T (for the SPARC-Collab.) “Stored Particle Atomic Physics Research Collaboration: Atomic Physics with Stored Highly-Charged Heavy Ions at the Future FAIR Facility”, [http://www-linux.gsi.de/~sparc/documents/pdf\\_files/sparc\\_stori05.pdf](http://www-linux.gsi.de/~sparc/documents/pdf_files/sparc_stori05.pdf)
81. Welsch C P, Grieser M, Ullrich J, Wolf A (for the FLAIR Collab.), FLAIR Project at GSI, International Workshop on Beam Cooling and Related Topics, COOL05, Galena, IL, USA (2005), [http://www.oaew.ac.at/smi/flair/pub/Cool05\\_FLAIR.pdf](http://www.oaew.ac.at/smi/flair/pub/Cool05_FLAIR.pdf)
82. Maury S, “The Antiproton Decelerator (AD)”, CERN/PS 99-50 (HP)
83. FAIR Baseline Technical Report, Vol. 2. Accelerator Facilities (2006) p. 471
84. The HITRAP decelerator and trap facility, [http://www.gsi.de/forschung/ap/projects/hitrap/index\\_e.html](http://www.gsi.de/forschung/ap/projects/hitrap/index_e.html)
85. Widmann E *Nucl. Phys. A* **752** 87 (2005)
86. Ellis J R et al. *Phys. Rev. D* **53** 3846 (1996)
87. Cellady D, Kostecky A *Phys. Rev. D* **55** 6760 (1997)
88. Bluhm R, Kostecky V A, Russel N *Phys. Rev. D* **57** 3932 (1998)
89. Walz J, Haensch T W *Gen. Relat. Grav.* **36** 561 (2004)
90. Weyrather W K *Int. J. Radiat. Biol.* **75** 1357 (1999)
91. Durante M, Cucinotta F A *Nature Rev. Cancer* **8** 465 (2008)
92. Curtis S B et al. *Adv. Space Res.* **22** (2) 197 (1998)
93. Bethe H A *Handbuch für Physik* Vol. 24/2 (Berlin: Springer-Verlag, 1933)
94. Curtis S B *Radiat. Measurements* **23** (1) 5 (1994)
95. Kraft M *Nucl. Sci. Appl.* **3** 1 (1987)
96. Kraemer M et al. *Rad. Environ. Biophys.* **33** 91 (1994)
97. Durante M *J. Radiat. Res.* (Tokyo) **50** (Suppl. A) A55-8 (2009)
98. Holmes-Siedle A, Adams L *Handbook of Radiation Effects* (Oxford: Oxford Univ. Press, 2002)
99. Haberer Th et al. *Nucl. Instrum. Meth. Phys. Res. A* **330** 296 (1993)
100. Marletta G, Bouffard S, Neumenn R (Eds) *Nucl. Instrum. Meth. Phys. Res. B* **209** 1 (2003)
101. Schwietz G et al. *Phys. Rev. Lett.* **69** 628 (1992)
102. Xiao G et al. *Phys. Rev. Lett.* **79** 1821 (1997)
103. BIOMAT Collab. “Letter of Intent for: Materials Research with Relativistic Heavy Ion Beams”, [http://www.gsi.de/fair/experiments/biomat/BIOMAT\\_LOI\\_Mat.pdf](http://www.gsi.de/fair/experiments/biomat/BIOMAT_LOI_Mat.pdf)
104. Kumbara T et al. *Nucl. Instrum. Meth. Phys. Res. B* **164–165** 415 (2000)
105. Kumbara T et al. *Nucl. Instrum. Meth. Phys. Res. B* **193** 371 (2002)
106. Geissel G, Scheidenberger C *Nucl. Instrum. Meth. Phys. Res. B* **136–138** 114 (1998)
107. Scheidenberger C, Geissel G *Nucl. Instrum. Meth. Phys. Res. B* **135** 25 (1998)
108. Stämmler Th et al. *Hyperfine Interact.* **106** 307 (1997)
109. Sturm C, Sharkov B, Stocker H *Nucl. Phys. A* **834** 682c (2010)